

(NASA-IM-81310) CONCEPTUAL/PRELIMINARY
DESIGN STUDY OF SUBSONIC V/VSTOL AND STOVL
AIRCRAFT DERIVATIVES OF THE S-3A (NASA)
64 p HC A04/5r A01

N81-29118

CSCJ JIC

Unclass
63/05 27070

Conceptual/Preliminary Design Study of Subsonic V/STOL and STOVL Aircraft Derivatives of the S-3A

George H. Kidwell, Jr.

July 1981



NASA
National Aeronautics and
Space Administration

Conceptual/Preliminary Design Study of Subsonic V/STOL and STOVL Aircraft Derivatives of the S-3A

George H. Kidwell, Jr., Ames Research Center, Moffett Field, California



National Aeronautics and
Space Administration

Ames Research Center
Moffett Field, California 94035

TABLE OF CONTENTS

	<u>Page</u>
ABSTRACT	1
INTRODUCTION	2
DESIGN PROCEDURE	
Design Synthesis Program	3
Design Procedure	8
DESIGN OF COMMON SYSTEMS	
Propulsion System	10
Nacelles	12
Wing Structure	12
Reaction Control System	13
Mission	15
AIRCRAFT DESIGNS AND THEIR PERFORMANCE	
Influencing Factors	16
Fixed Wing with Unconstrained Span	18
Fixed Wing with 64-Foot Span Constraint	19
Oblique Wing with Unconstrained Span	20
DESIGN ANALYSIS AND COMPARISON	
Design Analysis	22
Design Comparison	24
CONCLUSIONS	28
REFERENCES	29
TABLES	
Tab. 1 S-3A Geometric Data	31
Tab. 2 S-3A Weight Data	31
Tab. 3 Pegasus Engine Performance Data	32
Tab. 4 CFM-56 Engine Performance Data	32
Tab. 5 Composite Wing Weight Savings Buildup	32
Tab. 6 Geometric Data for S-3B Designs	33
Tab. 7 Weight Breakdown for S-3B Designs	33
Tab. 8 Unconstrained Span Available Control Power	34
Tab. 9 Constrained Span Available Control Power	34
Tab. 10 Oblique Wing Available Control Power	34
Tab. 11 Results of Intermediate S-3B Designs	35
Tab. 12 S-3B Mission Performance Results, Search and Attack Mission	36

	<u>Page</u>
Tab. 13 S-3B Mission Performance Results, other Missions . . .	37
Tab. 14 S-3B Tabular Performance Data	38
Tab. 15 S-3B/Pegasus Design Data	39

FIGURES

Fig. 1 Block Diagram of ACSYNT Program	40
Fig. 2 S-3A Search and Attack Mission Profile	41
Fig. 3 S-3A Surface Surveillance Mission Profile	42
Fig. 4 S-3A Combat Range Mission Profile	43
Fig. 5 S-3B Unconstrained Span Wing, Outline Drawing	44
Fig. 6 S-3B Unconstrained Span Wing, Range vs TOS	45
Fig. 7A S-3B Unconstrained Span Wing Sensitivity, Aspect Ratio	46
Fig. 7B S-3B Unconstrained Span Wing Sensitivity, Planform Area	46
Fig. 7C S-3B Unconstrained Span Wing Sensitivity, Taper Ratio	46
Fig. 7D S-3B Unconstrained Span Wing Sensitivity, Thrust/Weight	47
Fig. 7E S-3B Unconstrained Span Wing Sensitivity, Wing Weight Factor	47
Fig. 8 S-3B Constrained Span Wing, Outline Drawing	48
Fig. 9 S-3B Constrained Span Wing, Range vs TOS	49
Fig. 10A S-3B Constrained Span Wing Sensitivity, Aspect Ratio	50
Fig. 10B S-3B Constrained Span Wing Sensitivity, Planform Area	50
Fig. 10C S-3B Constrained Span Wing Sensitivity, Taper Ratio	50
Fig. 10D S-3B Constrained Span Wing Sensitivity, Thrust/Weight	51
Fig. 10E S-3B Constrained Span Wing Sensitivity, Wing Weight Factor	51
Fig. 11 S-3B Oblique Wing, Outline Drawing	52
Fig. 12 S-3B Oblique Wing, Range vs TOS	53
Fig. 13A S-3B Oblique Wing Sensitivity Aspect Ratio	54
Fig. 13B S-3B Oblique Wing Sensitivity Planform Area	54
Fig. 13C S-3B Oblique Wing Sensitivity Taper Ratio	54
Fig. 13D S-3B Oblique Wing Sensitivity Thrust/Weight	55
Fig. 13E S-3B Oblique Wing Sensitivity Wing Weight Factor	55
Fig. 14 S-3B / Pegasus Range vs TOS	56
Fig. 15A Summary of Range vs TOS Results - S-3B Unconstrained Span	57
Fig. 15B Summary of Range vs TOS Results - S-3B Constrained Span	58
Fig. 15C Summary of Range vs TOS Results - S-3B Oblique Wing	59

CONCEPTUAL/PRELIMINARY DESIGN STUDY OF SUBSONIC V/STOL
AND STOVL AIRCRAFT DERIVATIVES OF THE S-3A

George H. Kidwell, Jr.

Anies Research Center

ABSTRACT

A computerized aircraft synthesis program has been used to examine the feasibility and capability of a V/STOL aircraft based on the Navy S-3A aircraft. The design study focused on two major airframe modifications: replacement of the wing and substitution of Pegasus-like, deflected thrust, advanced technology turbofan engines in place of the S-3A's TF-34 engines. Three planform configurations for the all-composite wing were investigated: an unconstrained span design, a design with the span constrained to 64 feet, and an unconstrained span oblique wing design. Each design was optimized using the same design variables, and performance and control analyses were performed. The results indicate that, in addition to having vertical/short takeoff and landing capability, the mission performance of these V/STOL aircraft compares favorably with that of the CTOL S-3A. The oblique wing configuration was found to have the greatest potential in this application, because of its aerodynamic advantages and because it enables a large span wing to be compatible with small ships.

INTRODUCTION

NASA-Ames Research Center is NASA's lead Center for developing V/STOL research and technology, and is responsible for supporting those user organizations, military and/or civil, who are assessing V/STOL as candidate alternatives for future aircraft. Part of this support is in the form of developing fundamental and applied research and analyses directed toward increasing the data base in the areas of high- and low-speed aerodynamics, aircraft guidance and navigation, and flight dynamics and control. Another support aspect is to make available to government, industry, and university investigators, crucial research facilities. These include not only wind tunnels, flight simulators, computers, and other such ground-based installations, but also highly-versatile flight research aircraft. Although the latter are difficult to acquire, they provide valuable flight data for validating wind tunnel and analytical predictions, checking simulator fidelity, and developing other information which is otherwise not obtainable from ground-based facilities.

To generate a better understanding of the potential role that future V/STOL research aircraft can play in the development of needed V/STOL research and technology, NASA-Ames conducts in-house and contracted preliminary design and feasibility studies. One such study involved the low-cost approach of modifying an existing U.S. Navy S-3A by replacing the standard G.E. TF-34 engines with Rolls-Royce Pegasus vectored thrust engines of the type used in the British Harrier V/STOL aircraft, reference 1. A powerful reaction control system and other modifications would be incorporated to make this S-3A/Pegasus combination into a useful V/STOL flight research vehicle. Although a potentially useful research aircraft, the S-3A/Pegasus aircraft appears to be of limited usefulness in any of the known military/civil missions.

As a parallel to the conceptual study of combining Pegasus vectored thrust engines with an S-3A for research aircraft purposes, a companion study was conducted to evaluate the potential of the vectored thrust concept

as applied to S-3A derivative aircraft by examining the S-3A with a modified wing and with advanced vectored-thrust turbofan engines. In this study the usefulness of such a V/STOL concept was to be evaluated in terms of satisfying several known U.S. Navy mission needs currently satisfied by CTOL S-3A aircraft. The attractiveness of a modification to the S-3A to enable V/STOL flight would be a near-term subsonic V/STOL capability for the U.S. Navy at low-moderate cost and risk while retaining most of the existing S-3A vehicle and mission systems. This parallel conceptual design study of mission-oriented S-3A derivative V/STOL aircraft is the subject of this report.

Three aircraft configurations were examined: an unconstrained wing span design, a design with wing span constrained to 64 feet and an unconstrained span oblique wing design. All three configurations utilized the same advanced turbofan engine cycle with Pegasus-like thrust vectoring. This report describes the automated aircraft synthesis procedures used, the requirements and assumptions selected and the final optimized designs that evolved for the three aircraft configurations. The resultant conceptual designs are presented together with mission performance measures, design sensitivities and control characteristics. Comparisons of the designs are made with the S-3A aircraft and with each other.

DESIGN PROCEDURE

This section provides a description of how the design study configurations were derived. First will be a description of the conceptual/preliminary aircraft design computer program, ACSYNT. Secondly, the procedure used to produce the designs will be discussed.

Design Synthesis Program

The computerized synthesis program used as a design tool in this study was the Ames conceptual/preliminary aircraft design synthesis program (ACSYNT). This is a highly modularized system of subprograms, each responsible for either a control or an analysis function, see figure 1. When combined, these

form a very effective design/analysis program. This section will briefly describe the modules involved in this study. Detail will be greatly limited but references are cited for those having a further interest.

Control Program - The control or executive program controls the sequencing and information transfer for all of the other modules and handles the input to and the output from the entire synthesis program. It is where the program operational codes are specified, and also where the user defines the modules to be used, their order, and which are to input, execute, and output. For example, one typically wants the takeoff/landing module to read input data, then not to perform any execution at all during vehicle convergence, but to execute and output the results for the converged vehicle. This is possible because each module is divided into either three segments (input, execution, and output) or two (input, and execution/output, with the output turned on by a code), a calculation code from the control program determining which segment is performed. This format is the result of a requirement of the optimization routine whereby many subprograms are called for analysis many times, but these must only input and output once. The control program also features a convergence routine which begins with an assumed vehicle gross takeoff weight, makes a pass through the analysis modules using this weight to compute a new weight, then compares these and makes another guess at the starting weight. When convergence is achieved, it implies not only that the fuel weight is exactly the amount required for the mission, but also that the structural weight, wing area, engine size, etc. are based upon the true takeoff weight.

Optimization - Actually part of the ACSYNT Control Program, the optimization routine, COPES/CUNMIN, shown in references 2 and 3, is considered individually because it is a stand alone program which can be coupled to most any analysis program. There are many analysis functions available with this program, specifically: single analysis (simply a single execution pass through the analysis), optimization (values are found for specified variables, corresponding to the minimum of some specified parameter), sensitivity analysis (the changes in certain parameters for changes in chosen variables),

two-variable function space (to enable mapping a function of two variables), optimum sensitivity (a sensitivity analysis but each perturbation point is re-optimized), and approximate optimization (a technique to further reduce the number of analyses by saving the information from previous analyses and curve fitting). The optimization algorithm is based on Zoutendijk's method of feasible directions and approaches the optimum after very few analyses. The functions available with this program greatly assist the designer in design evaluation. Both the optimization and the sensitivity analysis features were used extensively in the course of this study.

Geometry-Module - The geometry module basically performs two functions in ACSYNT. First is to provide geometric definition for the entire airplane, based upon conventional geometric parameters, for use by the other modules. An example would be its definition of the wing chords, span, thicknesses, etc., based upon wing loading, aspect ratio, taper, sweep, and thickness ratio. Secondly, this module computes the necessary wing, nacelle, and fuselage dimensions and volumes, based on requirements for fuel, engine, equipment, and payload volumes. The fuselage is modeled as a Sears-Haack body for area ruling and is sized to maintain specified shape parameters (fineness ratios, base area) while satisfying the volume requirements.

Aerodynamics Module - This module consists of procedures to calculate the aerodynamic characteristics of aircraft configurations for a given mission altitude and Mach number. It is used by the trajectory and takeoff/landing modules to provide aerodynamic coefficients for mission analysis calculations. This module also furnishes a detailed output of aerodynamic characteristics for a range of altitudes and Mach numbers. The calculation procedures use both theoretical methods and empirical information presented in references 4 and 5. Aerodynamic characteristics are estimated for subsonic, transonic, and supersonic flow and the special features of canards and oblique wings are included. For example, the wave drag of the oblique wing is calculated using a procedure similar to that of reference 6

with adjustments based on a correlation with wind-tunnel tests, reference 7, and with more elaborate prediction methods, reference 8. This calculation technique gives the wave drag as a function of Mach number, wing thickness, wing sweep, and wing aspect ratio. This module produces accurate estimates of aerodynamic characteristics while using very little computer time. It does not, however, estimate ground effects.

Propulsion Module - The propulsion module is a one-dimensional cycle analysis developed by Morris, reference 9, which sizes the engine, and calculates the (design and off-design) engine performance and other characteristics at a specified altitude and Mach number. This module is also called by the trajectory and takeoff/landing modules. Additionally, this module estimates the engine weight and physical dimensions and calculates nacelle dimensions for use by aerodynamics. ACSYNT currently has six turbojet and turbofan engines modeled, but other engines may be used by inputting the engine cycle and dimensional characteristics. Correlations with several engines showed good agreement. Installation losses are also estimated, according to the analysis method of reference 10.

Trajectory Module - This module estimates the aircraft's performance in flying a user-specified mission and determines the fuel weight necessary for a particular aircraft to accomplish the mission. The fuel weight estimate is of primary importance to the vehicle convergence cycle. The trajectory module uses information accessed from the aerodynamics and propulsion modules. Reference 11 presents the methods used in this program.

Mass Properties Module - After the vehicle has been sized, the structural weight is calculated by relationships described from correlations of existing data for the weights of the various vehicle components. The program is described in reference 12. Estimates made by this module may be overridden by the user if the true weight is known. Similarly, weight scaling factors have been provided for all major components so that they may be correlated

to an existing aircraft. Such a case would represent a new component geometrically and structurally similar to that of the correlated aircraft, useful in many situations. Also, scaling factors which allow for technology advances, for each component, are included.

Takeoff/Landing Module - The newest addition to ACSYNT, this module was considered necessary because of the importance of these regimes to V/STOL aircraft. Whereas the trajectory module handled these phases using the usual few equations, the present module digitally simulates the flight mechanics using a step time integration and can thereby estimate takeoff and landing trajectories. The procedure used is similar to that of reference 13. Many features were included to enable the program to accurately predict aircraft trajectory paths based upon the given vehicle configuration and the user-specified propulsion and aerodynamic control commands.

A problem with this module is that the program's execution time is 2-3 times that of the usual convergence run. For this reason, usually (for takeoff) an estimate is made for the takeoff fuel required, the vehicle's weight is converged using this estimate, then the takeoff/landing module is executed. As the need arises, this module is continually being improved to handle new propulsive-lift concepts and new control tasks.

Additional information on the ACSYNT Program may be found in references 14 and 15. The accuracy of its methods generally produces a maximum error of 5 percent, good for a conceptual/preliminary design synthesis program. Its versatility has been demonstrated by correlations with a variety of aircraft, including the F-5E, C-5A, and Boeing 727. ACSYNT has been used in many performance analyses and design studies, of which references 16 - 20 are examples.

A second program was used in the analysis of each design to provide center of gravity (CG) and moment of inertia information. This program does require some detailed input, such as the longitudinal position of major equipment, but this information was available since a large portion of the

standard S-3A was used. Many calculations, such as the inertial effect of the wing fuel, are accurately estimated using a stripwise integration procedure. This information allowed rapid iteration of control system characteristics for the designs.

Design Procedure

There were two basic phases to this study. The first was the correlation of the design synthesis program with the S-3A. This provided a baseline, a model which could be modified and re-analyzed to estimate the effects on performance. The second phase was the actual development of the three designs. In this effort, the baseline not only provided a model from which developments could be made, but also it was a consistent measure of performance gains or losses. The following paragraphs will describe the methods involved in these two phases.

The goal of a correlation is a model which can accurately predict the aerodynamic, propulsive, weight, and performance characteristics of an aircraft. Using the synthesis program, aircraft data is input and, together with any necessary multipliers, adjusted until a close approximation to the actual aircraft is achieved. This same process is used to model an engine. Tables 1 and 2 present geometric and weight data, respectively, for the S-3A. Since the S-3A model was completed, it has been used for several other studies as well as the present one.

The second part of this study was of course to examine the potential for modifying the S-3A to achieve a viable V/STOL mission vehicle. This phase also was divided into two parts. The first of these was the design, or selection, of systems which were common to all three configurations, namely the engine, nacelles, wing structure, and reaction control system. This is not to imply that the same system was necessarily used for each design, but rather that all of the design decisions were made and then the system was sized as required. Decisions regarding the mission(s) were also made at this time.

With all of the secondary work completed, the final designs were synthesized with the aid of numerical optimization. Each final design was investigated using analyses of its performance sensitivities to geometric and mission changes.

The following two sections will discuss, in detail, the aforementioned design procedure. Both will show the specifications and constraints, the goals and guidelines, the assumptions, the design decisions, and the supporting data. The first section will deal with the common systems and the second will present the completed designs.

DESIGN OF COMMON SYSTEMS

This section will summarize the design history for the systems which were designed once, to be used for all three aircraft designs. These systems are the engine, nacelles, wing structure, and reaction control system (RCS).

The following format will be used for this discussion. First, all of the factors which concern the design will be listed. These factors include design specifications and constraints, the goal(s) of the design, assumptions which were made in the course of the design, physical limitations and so forth. Data will be presented, if possible, and the design decisions will be explained. Limitations of, or risks with, the chosen design will be examined.

It should be stated at the start that these aircraft were assumed to have an Initial Operational Capability (IOC) of about 1983; thus, current technology was used. Also, the general concept of modifying the S-3A for V/STOL capability will hereafter be referred to as the S-3B for ease of discussion.

Propulsion System

The choice of a propulsion system was the most critical aspect of these designs. While this is true for any VTOL aircraft, the problem was aggravated because for an ASW aircraft, mission effectiveness is proportional to fuel efficiency. Ordinarily, this would lead one to look at either turboprops or high bypass ratio turbofan engines, as these have the best specific fuel consumption characteristics. However, a major specification in this design study was that the propulsion system be restricted to vectored thrust engines, similar to the four nozzle design of the Rolls-Royce Pegasus. The Pegasus is a low bypass ratio turbofan which ducts fan air through the forward nozzles and core flow through the aft nozzles. Table 3 gives some of the characteristics of the Pegasus engine used in the AV-8B. The SFC characteristics are not suitable for an endurance-type airplane, primarily because of low bypass flow (this will be seen later by an S-3B design which would use this engine). As a result, although the Pegasus is the only production engine having a thrust vectoring capability, an alternative was necessary for use on the S-3B.

An advanced technology high-bypass ratio turbofan engine was subsequently chosen for the S-3B. The characteristics of this class of engine cycle made it ideal for an endurance airplane limited to moderate subsonic speeds. The example chosen for this study was the CFM International CFM-56. The characteristics of this engine, shown in table 4, are representative of the advanced technology turbofans now in development and in production. There were several assumptions associated with the choice of this engine (or more accurately, engine cycle), and these will now be discussed.

The first assumption was that a four-nozzle, split-flow-type thrust vectoring system (or a 3-nozzle variation) could be used with this engine. The concern was not altogether with the mechanical adaptation to the engine, but also whether the change in backpressure from the ducts would adversely

affect the cycle (primarily the low pressure ratio fan). However, any problem would most likely be solved by minor redesign and the assumption was judged reasonable.

The second assumption was also related to the engine cycle, but could potentially have more impact than the first. It was assumed that a minimum of 5% of the core flow could be taken from the high pressure compressor for use in the RCS. Five percent core bleed is the usual amount available from this type of engine, but it is taken from the low-pressure compressor to drive accessories. There are no known studies which have addressed the bleed-air capabilities of a high bypass ratio turbofan engine and this is an important area to future powered-lift aircraft. The extraction of air from the high-pressure side is not expected to cause any problem and the usual 10% thrust loss was assumed for 5% bleed. In fact, it was estimated that for short durations, 10% core flow bleed could be used for emergency control situations (this will be discussed in the RCS Section). It is, however, not expected that the full 5% bleed capability would be used very often or for very long duration, since little time is usually spent in hover and full control authority would not normally be needed (depending upon available control power).

It was also assumed that this engine could be uprated 25% to approximately 29,400 pounds static sea level thrust, at least for a short time as is done with the Pegasus. In so doing, its envelope was held constant to the dimensions of the standard CFM-56 and an engine thrust/weight ratio of 7 was used. Additional weight was added for the accessories.

With regard to the thrust vectoring system, one basic difference with that of the Pegasus was that a single aft nozzle was used rather than two side-mounted nozzles. The Harrier requires the side-mounted nozzle system because it uses a single Pegasus engine mounted in the mid-fuselage for balance. The application to the S-3B was different since the engines were

wing-mounted. The single aft nozzle would be lighter and more efficient, since the large bifurcated duct which splits the core flow would be eliminated. A total of 800 pounds was allowed for the weight of the entire thrust vectoring system. This compares to 400 pounds for the system in the Harrier. The system on the S-3B was larger than that on the Harrier (10,000 lbs. additional thrust per engine), but improved materials and the removal of the bifurcated duct was estimated to offset these gains.

Nacelles

The conceptual design emphasis for the nacelles was strictly for lowest weight, since the S-3B was to be a military airplane with no noise restrictions. Guidance for the design of low weight advanced composite nacelles was found from the QCSEE Program, reference 21, and the AMST Program (proprietary data). As a result, a nacelle quite similar to the composite frame and nacelle design of the QCSEE Program was adopted. In this concept, the fan frame is a graphite/epoxy structure that incorporates the fan casing, fan bypass stator vanes and core frame into one all-bonded structure. Reference 21 estimates that this design could save from 25% to 35% in weight over an equivalent metal frame. The nacelle was designed entirely of advanced composite materials. Sources suggest that if no information on load distribution or structural function is available for the nacelle/pylon system, assume an 18% weight saving. This was the weight savings assumed, though it is conservative. The total nacelle system weight was estimated to be 1650 pounds, an increase of 845 pounds over the S-3A nacelles for the 9,000 lb. thrust TF-34 engines.

Wing Structure

The wing structure was assumed to be constructed entirely of advanced composite materials. Other aspects of the wing design, such as the wing fold or the effect of thickness, will be discussed in the next section. The only concern here is the weight break given over a comparable design using conventional materials. Guidance was taken from references 22 and 23, but

it should be understood that the topic of composite weight savings is a subject of much debate. Table 5 presents a summary of the estimate of the wing weight savings due to the use of advanced composite materials. To be somewhat conservative, most of the weight savings were computed assuming the wing components used something less than 100% composites, although the actual wing was assumed to be wholly composite. Based upon S-3A proportions of component weight to total wing weight, these savings produce a total of 36% for the entire wing. This represents a conservative estimate and the detailed design would undoubtedly surpass this savings.

Reaction Control System

There were two types of systems considered for the S-3B for hover and low-speed control. Since there are effectively four thrusting points on the aircraft (one forward and one aft on each engine), the magnitude and/or direction of any two of them can be changed with respect to the others to produce control moments. This method was used only for the oblique wing configuration for two reasons. First, roll control response would be dependent on engine throttle response, which for large fan engines (without variable inlet guide vanes - the CFM-56 has no inlet guide vanes) is very slow. (This also implies difficulty in height control for all three.) Secondly, with this system thrust that is redirected or reduced to produce a couple is lost for lifting purposes, so that a cross-coupling with height control is inherent. The oblique wing configuration, however, was forced to use this system for roll, since the variable sweep wing did not permit an RCS to be used in the wing.

On the other hand, when bleed air is taken from the engines for reaction control, the lost engine thrust is partially recovered as lift from the reaction control jet thrust (if only downward control jets are used). The response of the reaction control system is also very high because of the low inertias associated with the system valving. The reaction control system is simpler than one manipulating the thrust vectors, but it is also heavier due to its high-pressure air ducting. With regard to the ducting, quite often

sufficient volume is not available within the wing structure for the necessary pipes. The duct size and weight is dependent upon the mass flow required and the delivery pressure (higher pressure reduces the duct diameter, but increases the required wall thickness). In application to the S-3B, however, it will be seen that wing volume was not a problem. Thus the reaction control system was chosen.

To estimate the RCS weight, the Harrier was used as an example, see reference 24. Since RCS bleed air for the Harrier also comes from the high-pressure compressor (though mass flow for the S-3B was 10% less), the same ducting and control valves were assumed. The Harrier's RCS weight was scaled up in proportion to the increased duct runs of the S-3B. The total system weight was estimated to be 300 pounds, 100 pounds more than that of the Harrier. The locations of the RCS nozzles are as in the Harrier, i.e. the wing tips, and nose and tail booms. For the oblique wing control system, weight was allowed for the pitch and yaw RCS, but no weight was added for roll control.

Control power was not specified for this study. Instead, the control power available using 5% and 10% bleed rates was computed for each completed design. It is questionable whether the engine could remain running or avoid damage with 10% bleed. This setting, however, would only be used for severe (emergency) control needs and would be of short duration. Therefore, this rate was considered to be available. For the oblique wing roll control system, control power in hover was determined by adding 17% thrust (max. thrust) to one side and subtracting 17% (which gives 67% max. thrust) from the other. Special ratings for the engines for emergency roll control could also be included if deemed necessary.

There were two circumstances for handling an engine out. If an engine fails at some time other than in hover, the aircraft is retrieved with a slow arrested landing (Fowler flaps are retained on the new wings for such a

case) using the S-3A carrier gear (retained in the S-3B; damage in the emergency landing process is acceptable). An engine failure in hover was considered nonsurvivable for the airframe and the only concern was to maintain attitude for long enough to allow the crew to eject. Many schemes are possible for this task, such as short duration rockets for moment control, on-board APU with turbo-compressor to boost RCS massflow (started prior to any hover situation), sensors to power down the other engine automatically, etc. It should be noted that only recently has a Harrier/AV-8A/AV-8B experienced an engine failure in hover and this was quite benign.

Mission

The CTOL S-3A performs several ASW missions. These include search and attack, contact investigation, surface surveillance, and combat range. For use as a design mission for the S-3B, the search and attack mission was chosen since it most fully represents the ASW objective. This mission, with typical S-3A performance data, is shown in figure 2. The S-3B design mission was a constant 458 nm. mission radius with loiter time used as the mission variable. The mission payload (2955 lbs) was also maintained so that the comparison of the loiter time between the S-3A and S-3B would indicate the performance penalty of providing VTOL capability. As will be discussed in the next section, short takeoff/ vertical landing (STOVL) performance was also estimated for this mission.

A variation of the search and attack mission was also investigated. Because of the high thrust/weight ratio of a VTOL airplane, higher cruise Mach numbers than for the S-3A was achievable. A study was therefore made for each of the final designs to examine the mission potential for a 0.85 dash out to the loiter station (instead of 0.65). This Mach number corresponds to just below the drag rise Mach number for the fuselage, which is very blunt.

For additional information, two other missions, surface surveillance and combat range, were examined. These missions represent pure loiter and pure cruise, respectively, and provide an interesting indication of how well each of the S-3B designs performed the two major ASW mission components. Figures 3 and 4 show these missions for the S-3A.

This concludes the discussion of the early design work. The following section will introduce the remaining design goals and describe the resulting designs. The performance of these designs will also be shown.

AIRCRAFT DESIGNS AND THEIR PERFORMANCE

This section will describe the completion of the S-3B designs. The majority of the discussion will concern the wing designs, since they were the major difference between aircraft designs, i.e., two with conventional fixed wings and one with an oblique wing. Each design was developed using the optimization capability of ACSYNT. These designs will be presented in the following order showing the development and performance of each: a fixed wing with an unconstrained span, a fixed wing with a constrained span of 64 feet, and an oblique wing with unconstrained span. Additional design and performance information will be given in the next section when design comparisons are made. However, before the designs are presented, the remaining influencing factors that have not yet been discussed will be given.

Influencing Factors

Probably the most important requirement in this study was that most of the S-3A remain unchanged. The S-3A fuselage, empennage, and landing gear were maintained. It was assumed that the S-3A electronics suite would be used, although obviously during an aircraft modification such as this, modern (lighter) electronic equipment would likely be fitted. Also a crew of four was retained although it seems likely that electronic advances would permit the deletion of a crewman, particularly for V/STOL aircraft. These two conservative estimates, combined with others which have been made, imply

that the estimated performance is probably a lower bound, with greater performance linked to the accuracy of the analysis. The S-3A catapult and arresting gear was also retained, for simplicity and to permit emergency arrested landings. Additionally, Fowler flaps were retained to aid in engine out recovery of the aircraft.

To prevent the designs from getting too large for some of the alternative V/STOL carrier ships (destroyers and comparable-sized ships were not considered), an upper limit of 49,000 pounds was placed on the gross vertical takeoff weight (WVGTO). Short takeoff weight was constrained to 52,600 pounds, a structural limit for the S-3A airframe. The gross vertical takeoff thrust/weight ratio was set at 1.20, allowing 10% for the thrust loss corresponding to maximum RCS bleed, and 10% for height control (vertical acceleration) and possible negative ground effects. Also, two minutes of full power was required at the end of the mission, in addition to the reserve of 5% mission fuel. This was to ensure a sufficient capability for situations where the landing task is more demanding than was simulated, such as with high crosswinds or a violently pitching deck.

An ultra-short takeoff performance capability (no more than 400 feet of deck roll) was required for overload conditions when the aircraft could not take off vertically. For this study, an overload condition was created by increasing the fuel weight. There were two mission analyses associated with the STOVL performance of the S-3B. One was to perform the ASW design mission to determine the extra loiter time available by loading extra fuel in drop tanks. The second was to increase the weight to the limit with fuel, and also to replace the payload with an equivalent weight of fuel and associated tankage. In other words, both STOVL configurations weighed the maximum allowable amount, but the second had nearly 3,000 lbs. more fuel. By fitting a removable fuel tank in the bomb bay, the entire amount of extra fuel (above VTO) can be carried internally. Of course without payload, the airplane can no longer perform the search and attack mission. This configuration has been termed AEW (Airborne Early Warning) for the purposes of this study. Such an aircraft could, in an emergency, be sent on long-range semi-AEW

missions, using its ASW electronics. Regardless of its mission usefulness, this STOVL arrangement indicates the maximum potential of the S-3B aircraft. The mission performance data will be presented in the design comparison section of this paper.

Fixed Wing with Unconstrained Span

This design synthesis was done to determine how well the S-3B could perform if unencumbered by constraints imposed due to ship limitations. This configuration serves as a bench mark to indicate the mission performance penalties associated with operating this aircraft from smaller ships. Such penalties will be shown in the design analysis and design comparison section of this paper.

The first design decision was to use a supercritical airfoil for the wing. This airfoil type has several advantages for use on the S-3B, most notably its tolerance to high thickness ratios (thickness/local chord) without a severe drag penalty. A thickness ratio of 18% was used for the S-3B, providing plenty of wing volume for both fuel and RCS ducting. An associated benefit of higher thickness ratios is the reduction in wing weight, since additional volume permits a larger (more efficient) wing structure. A further advantage of the supercritical airfoil is its delay of drag rise. This benefit, however, was only realized when the high speed (Mach number 0.85+) dash was used in the mission.

The wing was located so that its upper surface was flush with the top of the fuselage, as with the S-3A. This was to obtain maximum clearance for the engines and to utilize the same fuselage cutout as the S-3A, but this location also saves weight and internal volume. The engines were laterally positioned on the wing so that there was sufficient clearance for the inboard nozzles. Wing fold mechanisms were also included, just outboard of the engine.

The wing was optimized to maximize the loiter time for the 49,000 lb. gross vertical takeoff weight. A constraint was imposed that the wing have at least enough volume for the mission fuel and the RCS ducting. This is important since, due to the fact that there are no field length or maneuvering requirements, the wing loading is free to increase for a weight decrease. The design variables were wing aspect ratio, planform area, taper ratio, and sweep. Mission fuel available was determined by subtracting the airframe and payload weights from the 49,000 lb. limit.

The final optimized configuration is shown in figure 5, and column 1 of tables 6 and 7 lists some of its geometric and weight characteristics respectively. Figure 6 presents the S-3B range-time on station performance using this wing. With the weight fixed at 49,000 lbs, the sensitivity of loiter time available to aspect ratio, planform area, taper ratio, thrust/weight ratio, and wing weight savings due to the use of advanced composite materials are shown in figure 7. Table 8 presents the available control power and the static margin, at takeoff, for this configuration.

Fixed Wing with 64-Foot Span Constraint

To enable the S-3B to be compatible with some of the proposed V/STOL carrying ships, the wing span was constrained for this design. Operation aboard a DD963 destroyer (and similar ships) was not required, so a wing span limit of 64 feet was specified, corresponding to LHA-width flight decks. This capability corresponds to operation on half of the ships designated for potential V/STOL usage by the Navy. All other design aspects were the same as for the unconstrained design.

The resultant optimum configuration is shown in figure 8 and column 2 of tables 6 and 7 lists geometric and weight data. Figure 9 shows the range-time on station performance and figure 10 shows the sensitivity of loiter time to aspect ratio, planform area, taper ratio, thrust/weight ratio, and wing weight savings due to the use of composites. Table 9 presents the available control power and the static margin, at takeoff, for this configuration.

Oblique-Wing with Unconstrained Span

In recent years, the oblique-wing concept has been receiving continued research effort at Ames and as this is being written, the AD-1 oblique-wing flight research aircraft is undergoing flight testing at NASA-Dryden Flight Research Center. The aerodynamic advantages are variable sweep, that wave drag is significantly reduced by improved volume distribution, and that lift is more uniformly distributed along the aircraft's longitudinal axis. Another potential benefit was seen for the use of an oblique wing on the S-3B - a wing which could be large for efficient cruise but could be rotated nearly 90 degrees for terminal flight operations aboard small ships. This could also be said for the more conventional aft-swept variable sweep wing, but the oblique-wing has the structural advantage that it is a one-piece continuous structure. A contractor study indicated that the design of the wing pivot joint was not a problem and that its weight was reasonable. References 25-27 provide a summary of oblique-wing technology.

This design study considered the application of an oblique-wing to the S-3B. Because pivoting the wing decreases the span perceived during takeoff and landing operations, the design of the wing was unconstrained. With regard to the wing, two design decisions were made prior to optimization. A taper ratio of 0.30 was chosen to approximate an elliptical planform (important for this wing), and the thickness ratio was set at 12% (a recommended maximum). The remaining wing design variables, aspect ratio and wing area, were used for the optimization.

There were two other differences, besides the wing, between the oblique-wing design and the others. One was the engine location. Since the wing pivots almost 90 degrees (limited by the vertical stabilizer), the engines could not be attached to the wing and thus they were mounted on the fuselage. Two problems exist with this engine location, both related to the lateral closeness between engine and fuselage. These are interference between the inboard nozzles and the supporting structure, and impingement of the engine efflux on the aircraft further downstream. The interference is caused by

the engine mounting structure which attaches to the engine at its midpoint (unless a mounting from the top of the engine to the side of the fuselage were designed), exactly the location of the inboard forward nozzle. Elimination of the inboard nozzles would be desirable for this mounting location. The engine efflux problem is caused by the engine being mounted too close to the fuselage for their longitudinal position. The longitudinal location is determined by the center of gravity location, and for structural reasons, the engines are limited to small standoff distances (especially for such a large and heavy engine as the CFM-56). Canting of the engines slightly outboard would help, as would eliminating the inboard nozzles. However, the level of detail in ACSYNT is such that the performance analyses are not affected by these problems.

The second design difference was in the low-speed control system. As mentioned earlier, a method other than RCS was required (at least for roll), since the wing was pivoted at low speed. The solution was to maintain RCS for pitch and yaw and to use differential thrust for roll control. For single command roll control power, power settings of 100% and 67% (of maximum thrust) produced the maximum roll couple while maintaining height equilibrium.

It should be pointed out that the wing was not swept in any flight regime other than hover. This is due to the nature of the ASW mission and because of the bluntness of the S-3's fuselage, both which keep speeds enough below the drag rise Mach number to prevent sweeping the wing. The pivoting feature was solely to enable V/STOL operation aboard small ships. A fuselage of higher fineness ratio would serve to permit a more effective use of the high speed potential of the oblique wing, if there were a mission need.

The resultant optimum configuration is shown in figure 11, and column 3 of tables 6 and 7 lists some of its geometric and weight characteristics. Figure 12 gives the range-time on station performance and figure 13 shows

the sensitivity of available loiter time to aspect ratio and planform area, taper ratio, thrust/weight ratio, and wing weight savings due to composites. Table 10 presents the available control power and the static margin, at takeoff, for this configuration.

This concludes presentation of the optimized S-3B configurations. The following section will present further design analysis, including an examination of the reasons for choosing the final configuration and additional data on mission performance. Also in the next section will be comparisons of each design and with the S-3A.

DESIGN ANALYSIS AND COMPARISON

This section will examine the final designs in two ways. First, each design will be analyzed to determine the basis for choosing it as the optimum configuration. Secondly, the S-3B designs will be compared with each other and with the S-3A. This will establish the relative merits of each design and determine the penalties associated with providing a V/STOL capability.

Design Analysis

The three S-3B configurations have differences among themselves due to differences in design assumptions and component characteristics. For the unconstrained conventional wing design, there were no configuration decisions made prior to design optimization. The thickness ratio was held at 18% to reduce the optimization time since prior analyses had indicated the design tendency to drive to this value (decreased wing weight and improved lift-curve characteristics, with only a small drag increase due to the low Mach numbers used in the ASW missions). The constrained-span design configuration was only different from the unconstrained design in span, the span constraint simply causing a rearrangement of an equal planform area.

The characteristics of the oblique wing, and no other factors, resulted in a design significantly different from the others. It is useful to briefly examine the rationale of each S-3B design chosen as an optimum design.

Since there was no span constraint on the first planform design, it was driven toward an extremely cruise-efficient arrangement. The aspect ratio was driven very high to maximize the lift-to-drag ratio. Increasing aspect ratio also increases the wing weight, but up to the optimum, the fuel saving was always greater. The optimum aspect ratio for the drag is higher than it would normally be because the 35% wing weight saving for composite materials meant that only 65% of a weight penalty was realized. The wing planform area was reduced to the minimum (that volume required to contain the mission fuel) in order to reduce drag and wing weight. The taper ratio was driven to a value which is a compromise between the wing weight benefit of a low value of taper, and the reduced fuel usage of a taper ratio of around 0.35 (an elliptical planform approximation).

When the wing span was constrained to a maximum of 64 feet, the optimum configuration changed somewhat. By reducing the aspect ratio 18% and slightly decreasing the planform area, the span was reduced 8 feet. However, despite the constraint, for the same mission this design's WVGTO was less than 200 lbs. over that of the unconstrained design, since the aspect ratio is still high, albeit lower than that of the unconstrained design.

The oblique wing design is significantly different from the other two. Previous studies had indicated that the thickness ratio should be about 12% and that value was used. A taper ratio of 0.30 was chosen to approximate an elliptical lift distribution. The resultant wing configuration had a low aspect ratio (4.7) and a very high planform area (884 sq. feet). The initial design for the optimization process had an aspect ratio of 10 and a planform area of 600 sq. feet. The final design weighed 4592 lbs. less than this initial design, for the same mission. A weight breakdown shows that the optimized wing weighed 2724 lbs. less and that the mission fuel requirement

was 659 lbs. more. Aspect ratio is always a strong driver of wing weight, but examination of the oblique wing weight equations used in ACSYNT shows that (for a unit change in aspect ratio) a greater saving is achieved by an oblique wing than with a conventional wing. Similarly, the wing weight increases by the square root of the planform area. However, for a given aspect ratio, increasing the planform area increases the Reynolds Number (increasing chord) which leads to lower skin friction drag. Analysis has shown that this effect is significant, thus, part of the increased fuel usage, caused by the low aspect ratio and higher area, is countered and the overall influence is to increase the planform area. The optimum design point is where the weight-increasing and weight-decreasing effects become equal (in absolute value).

In order to further observe design trends, table 11 has been included. This table presents a series of runs which both compares designs and serves to more accurately indicate design sensitivities. It is only a sampling of the design space explored in this study. Wing aspect ratio, planform area, taper ratio, thickness ratio, sweep, cruise Mach number, and loiter time were used as variables.

Design Comparison

The subject S-3B designs were all developed to have a vertical takeoff gross weight of 49,000 pounds, thus to judge the designs we must compare the mission performances. Other factors, such as available control power, STOL performance, and deck handling can also be used to establish a ranking of the designs. By comparing the S-3B designs with the S-3A, the overall penalty for V/STOL can be determined.

There are two useful ways to look at the mission performance of the S-3B designs. One is to compare the minimum WVGTO for a constant mission, and the other to compare maximum loiter time for constant range and WVGTO. Table 12, line 1 presents the comparison for constant mission. This indicates not

only a substantial weight saving for the oblique wing design, but also that the span constraint on the conventional wing increased the weight by only 200 pounds. Also shown for comparison is the S-3A weight for a 2.0 hour loiter, 8,400 pounds less than that of the oblique wing. Table 12, line 2 presents this data in another way and shows the maximum mission loiter time possible for a 49,000 pound WVGTO. This indicates that the difference of 2,300 pounds for the oblique wing is worth an extra 0.5 hour of loiter time.

For STOVL operation, the weight was increased to 52,600 pounds (the S-3A structural limit) by adding external tanks with additional fuel. Table 12, line 3 shows the increment in loiter time associated with this added fuel. The oblique wing design reached 4.4 hours of loiter time in the STOVL mode. This compares to a 4.5 hour loiter with a weight of 43,450 pounds for the S-3A or as line 2 shows, 6.4 hours for 49,000 pounds. Again, there is an increase of approximately 8,400 pounds, for the same mission, to convert the S-3A to a V/STOL-capable aircraft with an oblique wing. Table 16, line 5 presents the loiter time for the STOVL AEW mission, representing the zero payload case. The STO deck run for all three designs was around 200 feet.

As previously mentioned, other missions and mission variations were performed with the optimized S-3B designs. This data is presented in table 13 for the S-3B designs and for the S-3A, where applicable. There are two items of special interest in this data. First is that the S-3B configurations, having fuel weights equal to that of the S-3A, equal or exceed the S-3A in range-TOS performance. This is essentially due to the improved wing design. Secondly, the fast dash to station at Mach 0.85 does not result in an unacceptable mission degradation, therefore, this capability could provide a useful option to mission planners. Were it not for the bluntness of the fuselage, the dash speed could be increased even further. Both of these mission results indicate that the S-3B concept has significant potential.

Table 14 presents the data from tables 12 and 13 in a form allowing comparison between the conventional wing design and the oblique wing design. Two conclusions can be readily drawn. The first is that the oblique wing design is better able to cruise at Mach 0.85. The second is that the conventional designs have better aerodynamic performance at Mach 0.65, as seen by the decreasing differences with increasing fuel available. The oblique wing design has a higher loiter time only because its lower wing structural weight allows more fuel, for constant weight. For equal fuel volumes, the oblique wing would have the poorer range-TOS performance.

The control power data, see tables 8 - 10, indicate marginal control power for all three designs, the roll control power being the most deficient. The problem is due to the low available bleed rate of the engine and the large engine masses on the wing (which also is carrying fuel). Unless the on-board APU is used during VTOL operations to enhance PCS available thrust, an alternate control method, such as fitting variable inlet guide vanes and using differential nozzles deflection, will be required. In addition, the static margin values indicate that all designs are neutrally stable and therefore requires very little control authority for the flight control system.

When an engine is lost during wing-borne flight, the S-3B can be recovered aboard one of the larger V/STOL carriers using the standard S-3A arresting gear. The minimum useable approach speed for the S-3A is 100.7 knots. Due to the large planform area of the oblique wing configuration, its stall speed is below 75 knots (with all stores and excess fuel dumped), thus the S-3B oblique wing could also approach at approximately 100 knots. The conventional wing S-3B designs have approach speeds around 108 knots. In all three cases, a satisfactory nonpowered-lift arrested landing can be made, at a standard sink rate and at a gross weight within the S-3A limit for maximum carrier landing gross weight.

With regard to deck handling, the S-3B oblique wing design can be seen to be clearly more favorable. The wing can be rotated as much as 80 degrees before striking the vertical stabilizer, corresponding to a width of less than 11 feet. However, due to excessive length of the aircraft once the wing is rotated, a fold mechanism is still necessary for clearance on the elevators and hanger deck. When folded, two or three S-3B oblique wing aircraft can occupy an LHA elevator at a time. Most other aircraft, including the S-3A and S-3B conventional wing designs, have folded spans of greater than 20 feet. The real operational advantage of the oblique wing can be seen by noting that when conventional wing designs land vertically, they require an actual landing zone with an area of the length by the span of the aircraft, whereas the oblique wing design requires a zone of the span by 11 feet. A great deal of flight deck space can be saved for this reason.

As a final comparison, a brief study was made of the application of advanced Pegasus (Rolls-Royce Pegasus F402-RR-402) engines to the S-3B in place of the CFM-56 engines. An unconstrained span wing was optimized to minimize WVGTO for a loiter time of one hour (the two hour loiter time would not permit a converged airplane with a weight below 65,000 lbs.).

The resultant aircraft is interesting in that it reflects a different set of priorities in the design strategy due primarily to the characteristics of the Pegasus engine. As discussed earlier, the Pegasus is a low-bypass ratio turbofan engine and it therefore has a much higher specific fuel consumption. The resulting wing has a much lower aspect ratio (see table 15) because the high fuel consumption masks the aerodynamic advantages of a higher impact ratio wing and the wing design is therefore more strongly driven by structural weight. Figure 14 shows the range - TOS plot for the S-3B/Pegasus design, showing that this is a very poor cruise/loiter airplane. For comparison, figure 15 presents a range-TOS summary of all of the configurations discussed in this report.

CONCLUSIONS

A computerized aircraft synthesis program has been used to examine the feasibility of V/STOL aircraft based on the S-3A ASW aircraft. Assumptions made in this study have been purposely conservative. The results have shown that a vectored thrust VTOL airplane with a suitably designed wing and advanced technology turbofan engines would have only one-third less loiter capability than the S-3A, and essentially the same mission performance in the STOVL mode. Conversely, for the same mission, the best of the V/STOL designs weighs 8,400 pounds (10% of TOGW) more than the S-3A. The penalty associated with achieving V/STOL capability in this manner is quite reasonable if the advantages of V/STOL performance are judged necessary for improving ASW effectiveness in the near term.

In this study, the oblique wing configuration has been shown to be advantageous for several reasons, despite the low cruise Mach number. The results also have shown that, in this application, there is no real benefit in using a very high wing aspect ratio, and that once the requirement for wing-borne takeoff and landing is removed, the wing area is typically reduced 30 percent, unless other factors are involved. A possible follow-on study would be the design of an ASW fuselage that would permit transonic dash capability, since the necessarily high thrust/weight ratio for this is inherent in the VTOL concept.

REFERENCES

1. Lampkin, B.A.: A Candidate V/STOL Research Aircraft Design Concept Using a S-3A Airframe and Two Pegasus 11 Engines. NASA TM-81204, May 1980.
2. Vanderplaats, G.N.: Conmin - A Fortran Program for Constrained Function Minimization - User's Manual. NASA TMX-62,282, 1973.
3. Vanderplaats, G.N.: Automated Optimization Techniques for Aircraft Synthesis. AIAA Paper 76-909, presented at AIAA Aircraft Systems and Technology Meeting, Dallas, Texas, September 27-29, 1976.
4. Axelson, J.A.: Estimation of Transonic Aircraft Aerodynamics to High Angles of Attack. AIAA Paper 76-996, presented at AIAA 1976 Aircraft Systems and Technology Meeting, Los Angeles, Calif., August 4-7, 1975.
5. Axelson, J.A.: AEROX - Computer Program for Transonic Aircraft Aerodynamics to High Angles of Attack. NASA TMX-73,208, 1977.
6. Jones, R.T.; and Cohen, D.: Aerodynamics of Wings at High Speeds. In: Aerodynamic Components of Aircraft at High Speeds, Eds.: A.F. Donovan and H.R. Lawrence, Vol. VII, Princeton Univ. Press, 1957.
7. Graham, L.A.; Jones, R.T.; and Boltz, F.W.: An Experimental Investigation of an Oblique-Wing and Body Combination at Mach Numbers Between 0.60 and 1.40. NASA TMX-62,207, 1972.
8. Woodward, F.A.; Tinoco, E.N.; and Larsen, J.W.: Analysis and Design of Supersonic Wing-Body Combinations, Including Flow Properties in the Near Field, Part I: Theory and Application. NASA CR-73106, 1967.
9. Morris, S.J.: Gas Turbine Cycle Analysis Program for Use in Aircraft Synthesis. Presented at the Computer-Aided Design Workshop, NASA-Ames Research Center, Moffett Field, Calif., Jan. 23-24, 1975.
10. Morris, S.J.; Nelms, W.P., Jr.; and Bailey, R.O.: A Simplified Analysis of Propulsion Installation Losses for Computerized Aircraft Design. NASA TMX-73,136, 1976.
11. Tauber, M.E. and Patterson, J.A.: Trajectory Module of the NASA-Ames Research Center Aircraft Synthesis Program ACSYNT. NASA TM 78497, 1978.
12. Barlow, A.V. and Nelms, W.P., Jr.: Weight Estimating Relationships for Conceptual Aircraft Design. Unpublished NASA proprietary report, May 1977.
13. Bowles, J.V. and Galloway, T.L.: Computer Programs for Estimating Aircraft Takeoff and Landing Performance. NASA TMX-62,333, 1973.

14. Vanderplaats, G.N.: ACSYNT Program Overview. Presented at the Computer-Aided Design Workshop, NASA-Ames Research Center, Moffett Field, Calif., Jan. 23-24, 1975.
15. Gregory, T.S.: Computerized Preliminary Design at the Early Stages of Vehicle Definition. Presented at AGARD 43 Flight Mechanics Panel Symposium on Aircraft Design Integration and Optimization, Florence Italy, October 1-4, 1973, NASA TMX-62303.
16. Nelms, W.P., Jr., and Axelson, J.A.: Preliminary Performance Estimates of a Highly Maneuverable Remotely Piloted Vehicle. NASA TN D-7551, 1974.
17. Nelms, W.P., Jr., and Bailey, R.O.: Preliminary Performance Estimates of an Oblique, All-Wing Remotely Piloted Vehicle for Air-To-Air Combat. NASA TN D-7731, 1974.
18. Levin, A.D.; Castellano, C.R.; and Hague, D.S.: High Performance Dash on Warning Air Mobile Missile System. NASA TMX-62,479, 1975.
19. Vanderplaats, G.N., and Gregory, T.J.: A Preliminary Assessment of the Effects of Advanced Technology on Supersonic Cruise Tactical Aircraft. Presented at the Super Cruise Military Aircraft Design Conference, Colorado Springs, Colorado, February 17-20, 1976.
20. Nelms, W.P., Jr., Murphy, R.; and Barlow, A.: Preliminary Analysis of Long-Range Aircraft Designs for Future Heavy Airlift Missions. NASA TMX-73,131, 1976.
21. Stotler, C.L.: OCSEE Composite Frame and Nacelle. Presented at the Quiet Powered-Lift Propulsion Conference, held at Cleveland, Ohio, on 14-15 November, 1978.
22. Forsch, Hans H. (Grumman Aerospace): The Use of Advanced Composites in Aircraft Design. Presented at the Annual Aircraft Design Short Course, University of Dayton, Dayton, Ohio, July 12-15, 1976.
23. Nicolai, L.M.: Fundamentals of Aircraft Design. University of Dayton, Dayton, Ohio, p. 20-20.
24. Fozard, J.W.: The British Aerospace Harrier - Case Study in Aircraft Design. Presented at the AIAA Professional Study Series Five Case Studies in Aircraft Design, Washington, D.C., July 1978.

TABLE 1. - S-3A GEOMETRIC DATA

<u>WING</u>	
Planform Area (ft. ²)	598.0
Aspect Ratio	7.73
Span (ft.)	68.7
Taper Ratio	0.25
Thickness Ratio, Root	0.16
Thickness Ratio, Tip	0.12
Sweep, C/4 (deg.)	15.0
Mean Aero. Chord (ft.)	9.85
Root Chord (ft.)	14.08
Tip Chord (ft.)	3.5
Wing Loading (lb./ft. ²)	70.0
<u>GENERAL</u>	
Length (ft.)	53.3
Height (ft.)	22.75
Fuselage Length (ft.)	49.25
Fuselage Diameter (ft.)	8.3
Volume Coefficient, h. tail	0.632
Volume Coefficient, v. tail	0.062

TABLE 2. - S-3A GROUP WEIGHT DATA
(All Quantities in Lbs.)

Airframe	13,817
Wing	4,890
Propulsion	3,625
Fixed Equipment	10,044
Payload	3,675
Fuel	13,142
Gross Takeoff Weight	44,303

TABLE 3. - PEGASUS F402-RR-402 ENGINE DATA

Type	Two Spool Turbofan
Bypass Ratio	1.34
Overall Pressure Ratio	13.7
Max. EGT (°F)	2,195
Diameter (in.)	48.0
Length, Including Nozzles (in.)	140.9
Weight, Including Nozzles (lb.)	3,653
Thrust, Max. Static Sea Level	[SFC], (lb. [lb./hr./lb.])
Short Lift, Water Inj.	20,930 [0.764]
Normal Lift, Water Inj.	20,395 [0.756]
Short Lift, Without Water Inj.	19,917 [0.700]
Normal Lift, Without Water Inj.	19,018 [0.687]

TABLE 4. - CFM-56 ENGINE DATA

Type	Two Spool Turbofan
Bypass Ratio	6.0
Overall Pressure Ratio	25.0
Max. EGT (°F)	2300
Diameter (in.)	71.4
Length, Without Nozzle (in.)	95.7
Weight, Dry, Without Nozzle (lb.)	4410
Thrust, Max. Static Sea Level	[SFC], (lb. [lb./hr./lb.])
	22,000 (0.36)
Thrust, 30,000 ft., M = 0.50	[SFC], (lb. [lb./hr./lb.])
	5,700 (0.66)

TABLE 5. - COMPOSITE WING WEIGHT SAVINGS BUILDUP

<u>Component</u>	<u>% Composite by Weight</u>	<u>% Weight Saving</u>
Wing Box	80	35
Outer Skin	98	30
Ailerons	90	50
TE Flaps	90	50
LE Flaps	90	40
Spoilers	90	40
$\frac{\text{Wing Weight With Composites}}{\text{Wing Weight Without Composites}} = 0.65$		

TABLE 6. - S-3b GEOMETRIC CHARACTERISTICS

<u>Wing Parameters</u>	<u>Oblique Wing</u>	<u>Unconstrained</u>	<u>Constrained</u>
Planform Area (ft. ²)	884	474	453
Aspect Ratio	4.7	10.9	8.9
Span (ft.)	64.5	71.8	63.3
Taper Ratio	0.3	0.3	0.3
T/C, Root	0.12	0.18	0.18
T/C, Tip	0.12	0.18	0.18
Sweep, C/4 (deg.)	0	0	0
Mean Aero. Chord (ft.)	15.0	7.2	7.8
Root Chord (ft.)	21.1	10.2	11.0
Tip Chord (ft.)	6.3	3.0	3.3
W/S (lb./ft. ²)	55	103	108

TABLE 7. - S-3B WEIGHT SUMMARY
(All Quantities in Lbs.)

<u>Component</u>	<u>Oblique Wing Design</u>	<u>Unconstrained Span Design</u>	<u>Constrained Span Design</u>
Airframe	10,906	12,794	12,409
Wing	1,744	3,023	2,638
Propulsion	10,589	10,589	10,589
Fixed Equipment	11,144	11,144	11,144
Fuel	12,694	10,807	11,184
Payload	3,675	3,675	3,675
Gross VTO Weight	49,000	49,000	49,000
STOVL/ASW Fuel	15,986	14,098	14,483
STOVL/AEW Fuel	19,660	17,773	18,158
Gross STO Weight	52,600	52,600	52,600

TABLE 8. - UNCONSTRAINED-SPAN DESIGN AVAILABLE CONTROL POWER
(5% Bleed/10% Bleed)

<u>Maximum Angular Acceleration</u> rad/sec ²	<u>Mission Configuration</u>	
	V/TOL	STOVL
Pitch Axis	0.34/0.69	0.31/0.62
Roll Axis	0.48/0.96	0.38/0.75
Yaw Axis	0.32/0.64	0.27/0.55
Static Margin	1%	0

TABLE 9. - CONSTRAINED-SPAN DESIGN AVAILABLE CONTROL POWER
(5% Bleed/10% Bleed)

<u>Maximum Angular Acceleration</u> rad/sec ²	<u>Mission Configuration</u>	
	V/TOL	STOVL
Pitch Axis	0.35/0.70	0.31/0.63
Roll Axis	0.48/0.96	0.48/0.96
Yaw Axis	0.30/0.60	0.26/0.51
Static Margin	0	0

TABLE 10. - OBLIQUE WING DESIGN AVAILABLE CONTROL POWER
(5% Bleed/10% Bleed)

<u>Maximum Angular Acceleration</u> rad/sec ²	<u>Mission Configuration</u>	
	V/TOL	STOVL
Pitch Axis	0.37/0.75	0.34/0.69
Roll Axis	0.67	0.57
Yaw Axis	0.39/0.77	0.27/0.54
Static Margin	0	1%

TABLE 11. - COMPARISON OF S-38 GROSS VERTICAL TAKEOFF WEIGHT VERSUS S-38 DESIGN VARIABLES

λ	t/c	$A_c/4$ deg.	M_{cruise}	t_{loiter} , minutes	Oblique Wing Design (lb.)	Unconstrained Span Design (lb.)	Constrained Span Design (lb.)
0.2	0.12	0	0.65	120	46,700	48,412	48,430
0.3			0.65	120	46,736	48,236	48,265
0.2			0.85	120	46,787		
0.3			0.85	120	46,824		
0.2			0.65	180	49,135		
0.3			0.65	180	49,184		
0.2			0.85	180	49,228	50,970	50,977
0.3			0.85	180	49,277		
0.3			0.18	0	0.65	120	48,032
0.2			0.65	120	48,174	48,340	
0.3			0.85	180	51,825		
0.3			0.85	180	51,952		
0.2			0	180	51,974		
0.3			0	120	48,985	48,986	
0.3			0	180	50,560	51,203	

TABLE 12. - LOITER PERFORMANCE COMPARISON SEARCH AND ATTACK MISSION

CONSTANT (VALUE)/VARIABLE (UNITS)	VALUE OF VARIABLE			
	S-3B Oblique Wing	Unconstrained Span	S-3B Constrained Span	S-3A
Loiter Time (2.0 hrs)/WVGTO* (lbs)	46,700	48,032	48,204	38,223
WVGTO (49,000 lbs)/Loiter Time (hrs)	3.3	2.4	2.3	6.4
ASW WGT0 (52,600 lbs)/Loiter Time (hrs)	4.4	3.6	3.4	-
AEW WGT0 (52,600 lbs)/Loiter Time (hrs)	6.2	5.4	5.1	-

* Gross Vertical Takeoff Weight

TABLE 13. - S-3B ALTERNATE MISSION PERFORMANCE

Mission	Oblique Wing Design	Aircraft Unconstrained Span Design	Constrained Span Design
Search and Attack, VTOL, M = 0.85 in Cruise	3.2	<u>Loiter Time, Hrs</u> 1.9	2.0
Search and Attack, STOVL (ASM), M = 0.85 in Cruise	6.4	3.2	2.8
Search and Attack, STOVL (AEM), M = 0.85 in Cruise	6.2	5.1	4.5
Combat Range, VTOL	2175	<u>Range, NM</u> 1825	1784
Combat Range, STOVL (AEM)	3427	3074	2945
Surface Surveillance, VTOL	5.3	<u>Loiter Time, Hrs</u> 4.5	4.4
Surface Surveillance, STOVL (ASM)	6.4	5.7	5.4
Surface Surveillance, STOVL (AEM)	8.1	7.4	7.0

TABLE 14. - S-3B MISSION PERFORMANCE COMPARISON

MISSION, AIRCRAFT CATEGORY	S-3B DESIGN	RANGE, NM	% DIFFERENCE*
Combat Range, VTOL	Oblique Wing	2175	-
	Unconstrained Span	1825	-16
	Constrained Span	1784	-18
	Oblique Wing	3427	-
	Unconstrained Span	3074	-10
Combat Range, AEW STOVL	Constrained Span	2945	-14
MISSION, AIRCRAFT CATEGORY	S-3B DESIGN	LOITER TIME, MINUTES	% DIFFERENCE*
Search and Attack, VTOL	Oblique Wing	195	-
	Unconstrained Span	143	-27
Search and Attack, ASW STOVL	Constrained Span	137	-30
	S-3A	383	96
Search and Attack, AEW STOVL	Oblique Wing	264	-
	Unconstrained Span	216	-18
Search and Attack, VTOL**	Constrained Span	204	-23
	Oblique Wing	371	-
Search and Attack, ASW STOVL**	Unconstrained Span	325	-12
	Constrained Span	306	-17
Search and Attack, AEW STOVL**	Oblique Wing	193	-
	Unconstrained Span	115	-40
Search and Attack, AEW STOVL**	Constrained Span	120	-37
	Oblique Wing	263	-
Search and Attack, AEW STOVL**	Unconstrained Span	193	-26
	Constrained Span	166	-37
Search and Attack, AEW STOVL**	Oblique Wing	370	-
	Unconstrained Span	304	-18
Constrained Span	271	-27	

* % Difference Compared to Oblique Wing Design Performance

** M = 0.85 in Cruise (Compared to M = 0.65 Otherwise)

TABLE 15. - S-3B/PEGASUS DESIGN DATA

- T/W = 1.06
- Optimized for Maximizing Loiter Time of Search and Attack Mission for Range of 916 NM

<u>WING</u>	
Planform Area (ft. ²)	535.7
Aspect Ratio	7.18
Span (ft.)	62.0
Taper Ratio	0.3
Thickness Ratio, Root	0.18
Thickness Ratio, Tip	0.18
Sweep, c/4 (deg.)	0
Mean Aerodynamic Chord (ft.)	9.5
Root Chord (ft.)	13.3
Tip Chord (ft.)	4.0
W/S	91.5

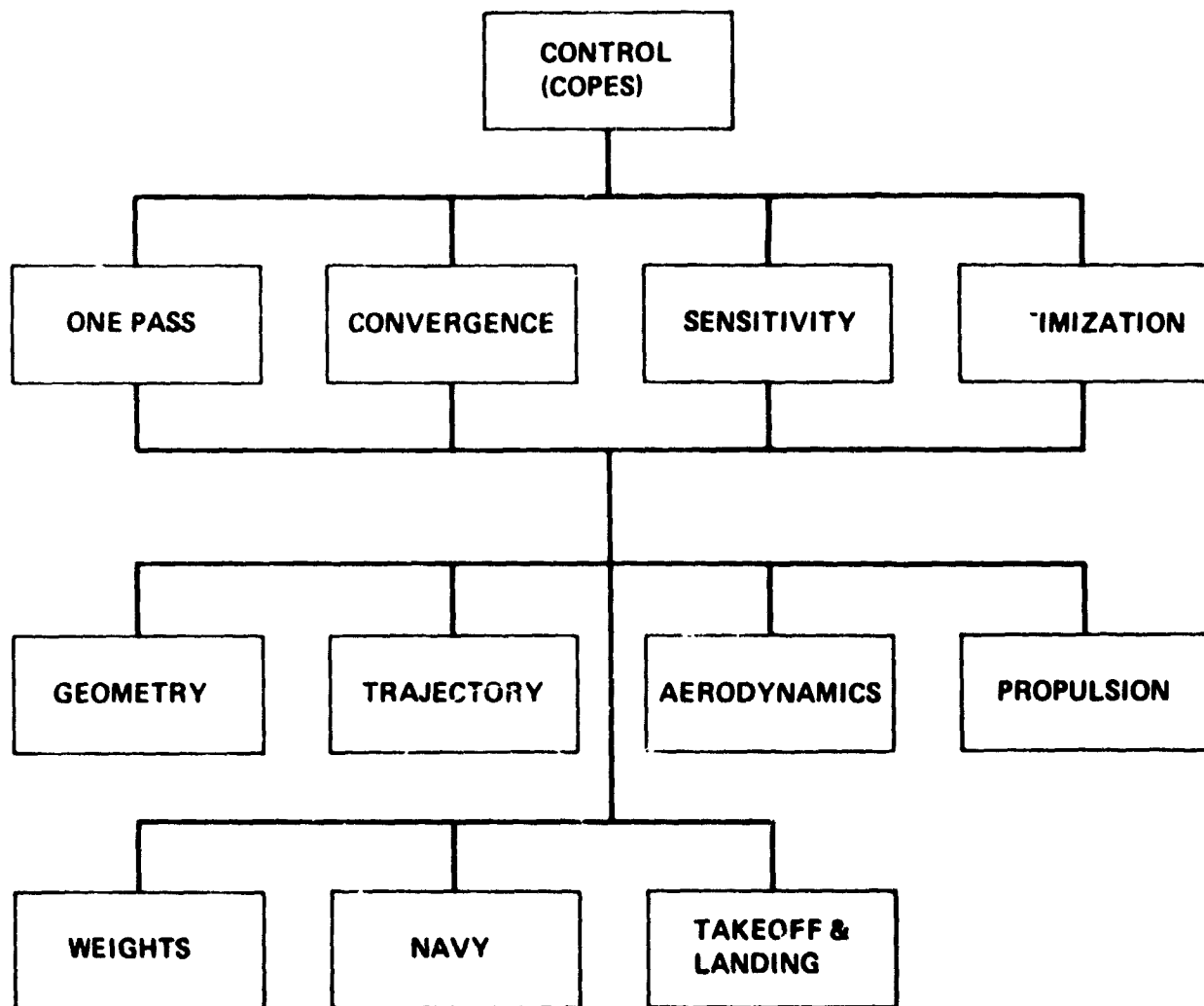
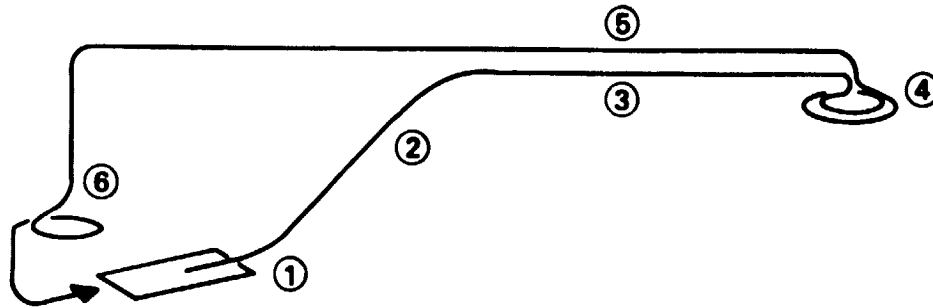
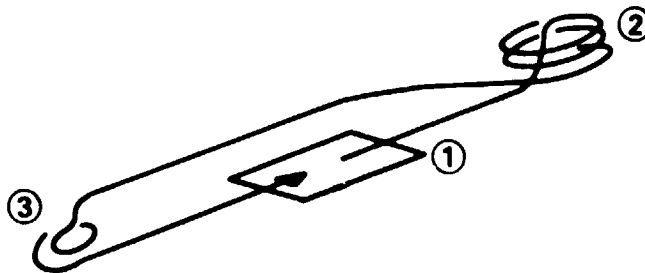


Figure 1. - Block Diagram of ACSYNT Program



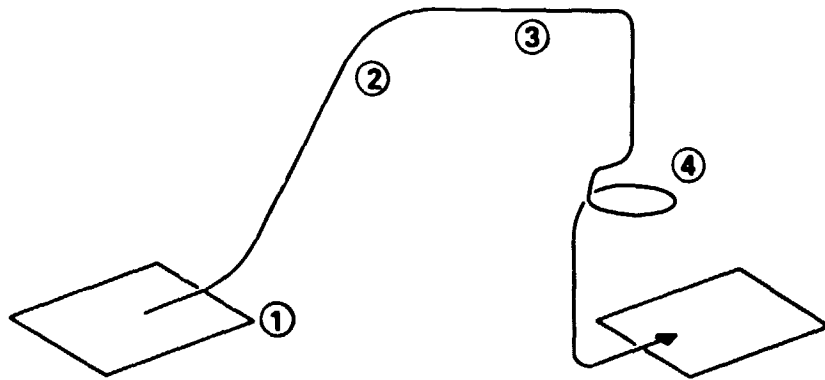
ITEM	INITIAL WEIGHT, (lb)	POWER SETTING	AVG. SPEED, (knots)	INIT. ALT., (ft)	TIME, (hr)	FUEL, (lb)	DIST., (n.mile)
1. WARM-UP & TAKEOFF	43449	MAX CONT	—	0	0.08	427	—
2. CLIMB	43022	INTER	—	0	0.36	1176	110
3. CRUISE OUT AT OPTIMUM ALTITUDE	41846	PART	356	37806	0.97	1636	348
4. LOITER ON STATION	40210	PART	370	40000	4.50	7069	—
5. CRUISE BACK AT OPTIMUM ALTITUDE	33140	PART	344	40000	1.33	1732	458
6. RESERVE LOITER	31407	PART	155	0	0.33	445	—
5% INITIAL FUEL	30963	—	—	—	—	657	—
TOTALS:							
MISSION TIME (ITEMS 2 THROUGH 5)			7.16 hr				
MISSION FUEL (ITEMS 1 THROUGH 5)			12040 lb				
FUEL LOAD			13142 lb				
RADIUS			458 n.mile				

Figure 2. - S-3A Search and Attack Mission Profile



ITEM	INITIAL WEIGHT, (lb)	POWER SETTING	AVG. SPEED, (knots)	INIT. ALT., (ft)	TIME, (hr)	FUEL, (lb)	DIST., (n.mile)
1. WARM-UP & TAKEOFF	43449	MAX CONT	-	0	0.08	427	-
2. LOITER ON STATION AT S.L.	43022	PART	165	0	7.70	11615	-
3. RESERVE LOITER	31407	PART	155	0	0.33	445	-
5% INITIAL FUEL	30963	-	-	-	-	657	-
TOTALS:							
MISSION TIME (ITEM 2)		7.70 hr					
MISSION FUEL (ITEMS 1 AND 2)		12040 lb					
FUEL LOAD		13142 lb					

Figure 3. - S-3A Surface Surveillance Mission Profile



ITEM	INITIAL WEIGHT, (lb)	POWER SETTING	AVG. SPEED, (knots)	INIT. ALT., (ft)	TIME, (hr)	FUEL, (lb)	DIST., (n.mile)
1. WARM-UP & TAKEOFF	43449	MAX CONT	—	0	0.08	427	—
2. CLIMB	43022	INTER	—	0	0.36	1176	110
3. CRUISE OUT AT OPTIMUM ALTITUDE	41846	PART	356	37806	7.07	10437	2089
4. RESERVE LOITER	31407	PART	155	0	0.33	445	—
5% INITIAL FUEL	30963	—	—	—	—	647	—
TOTALS:							
MISSION TIME (ITEMS 2 AND 3)			7.43 hr				
MISSION FUEL (ITEMS 1 THROUGH 3)			12040 lb				
FUEL LOAD			13142 lb				
RANGE			2628 n.mile				

Figure 4. - S-3A Combat Range Mission Profile

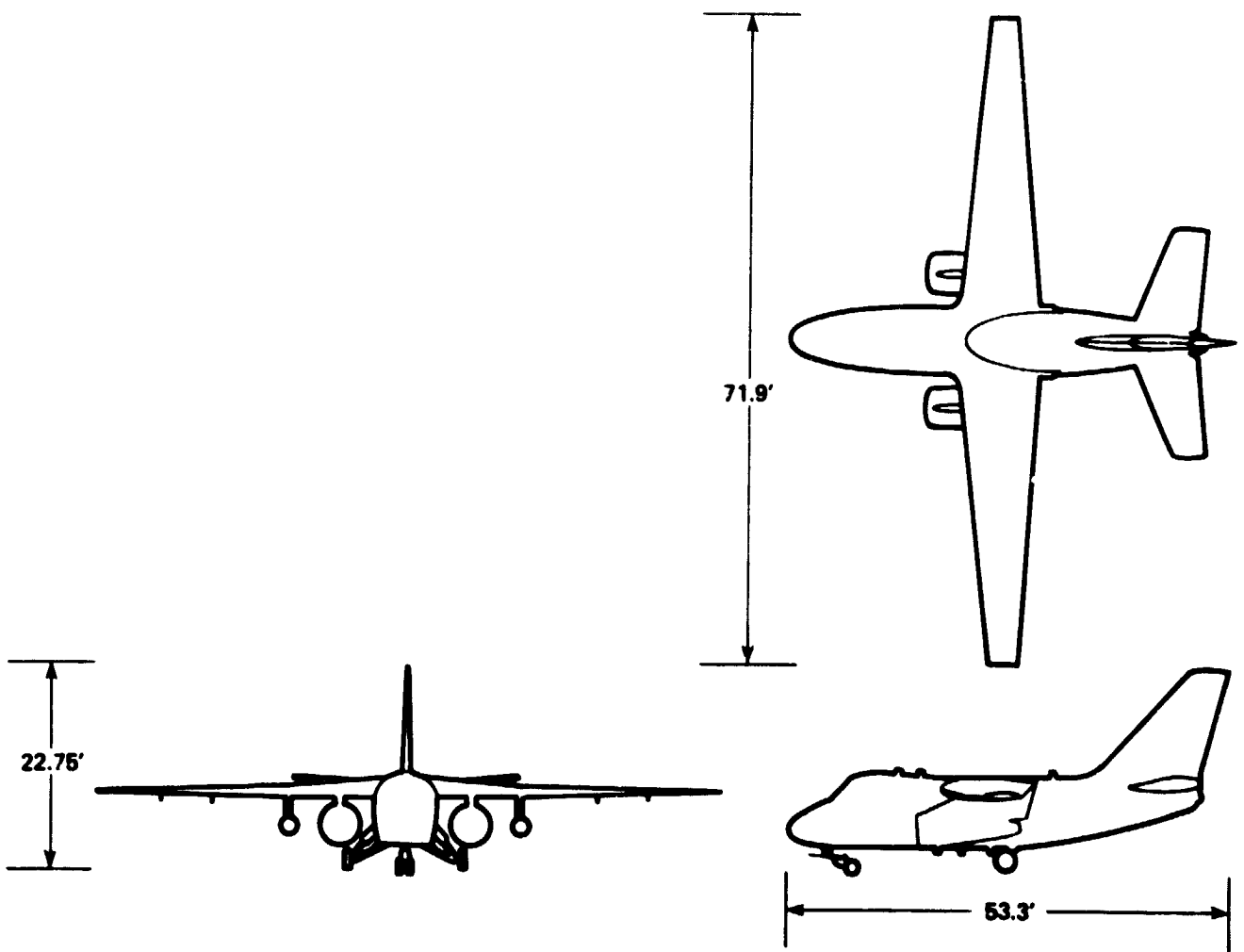


Figure 5. - S-38 Unconstrained Span Design Outline Drawing

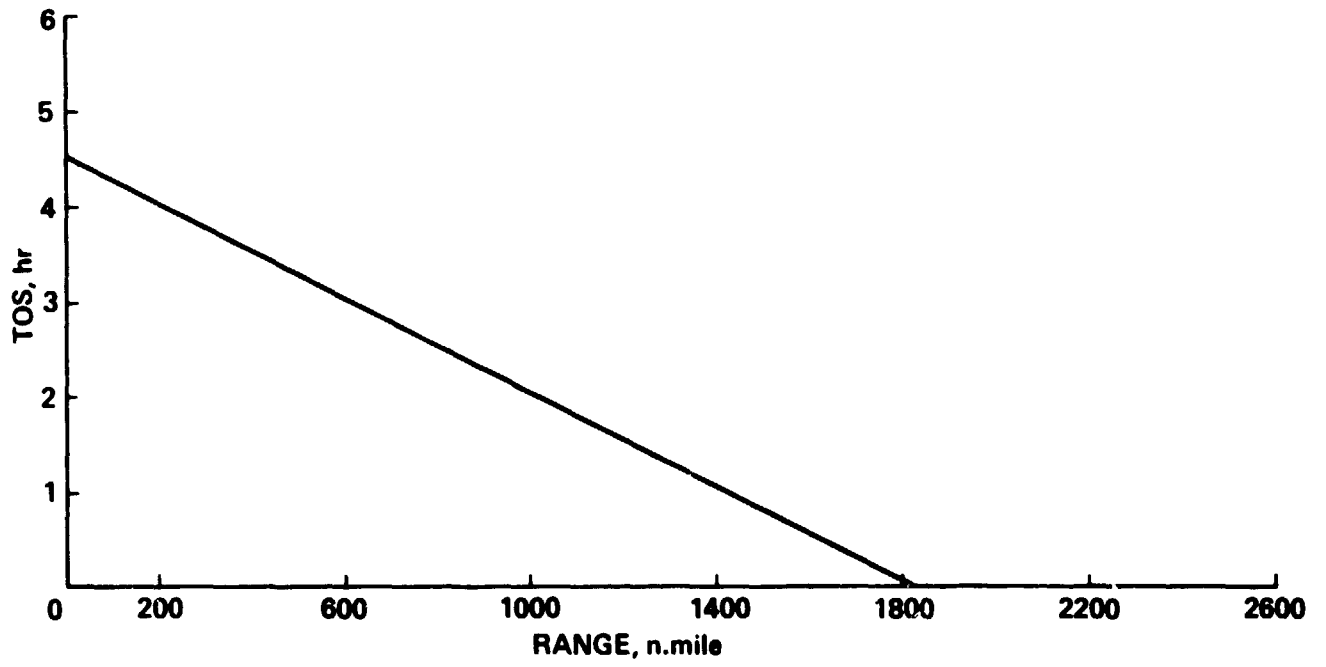


Figure 6. - Unconstrained Spar Wing Design Range Vs. Time in Station

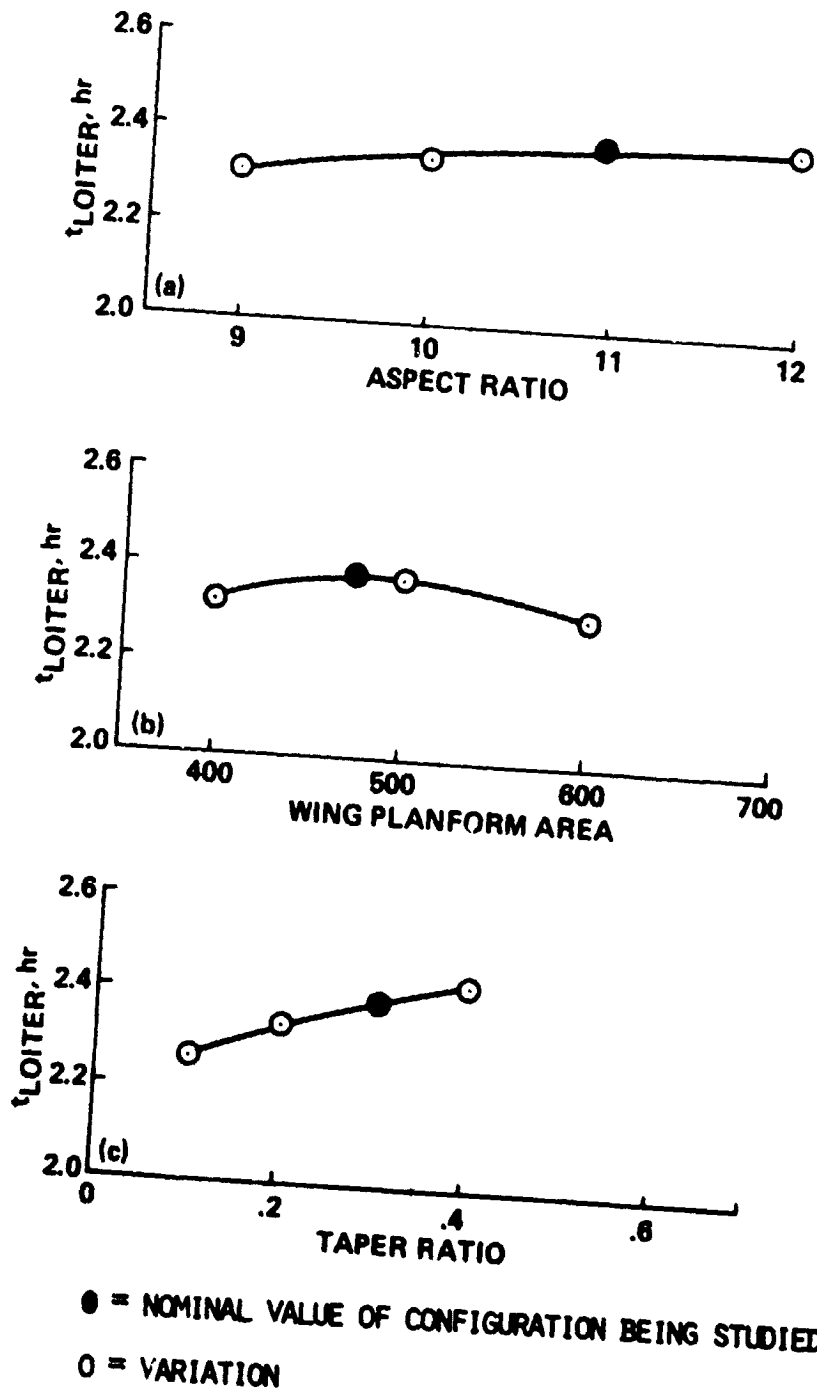
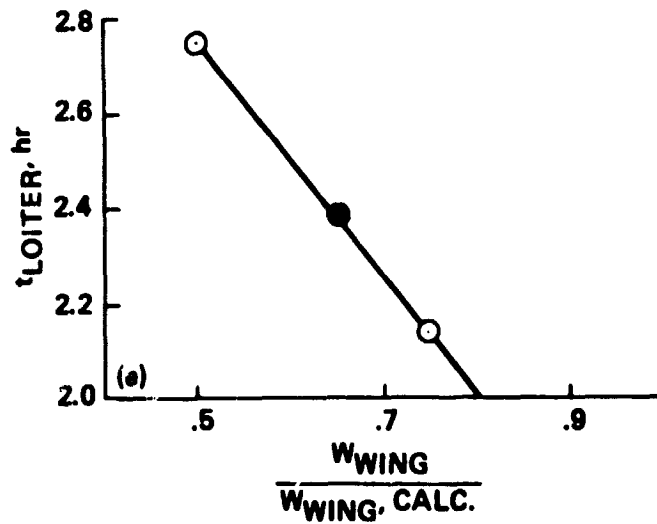
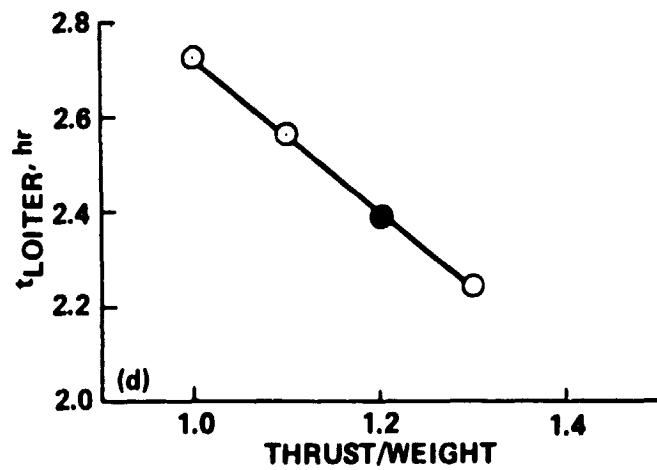


Figure 7. - Unconstrained Span Wing Design Loiter Sensitivity



● = NOMINAL VALUE OF CONFIGURATION BEING STUDIED
 ○ = VARIATION

Figure 7 (Cont'd). - Unconstrained Span Wing Design Loiter Sensitivity

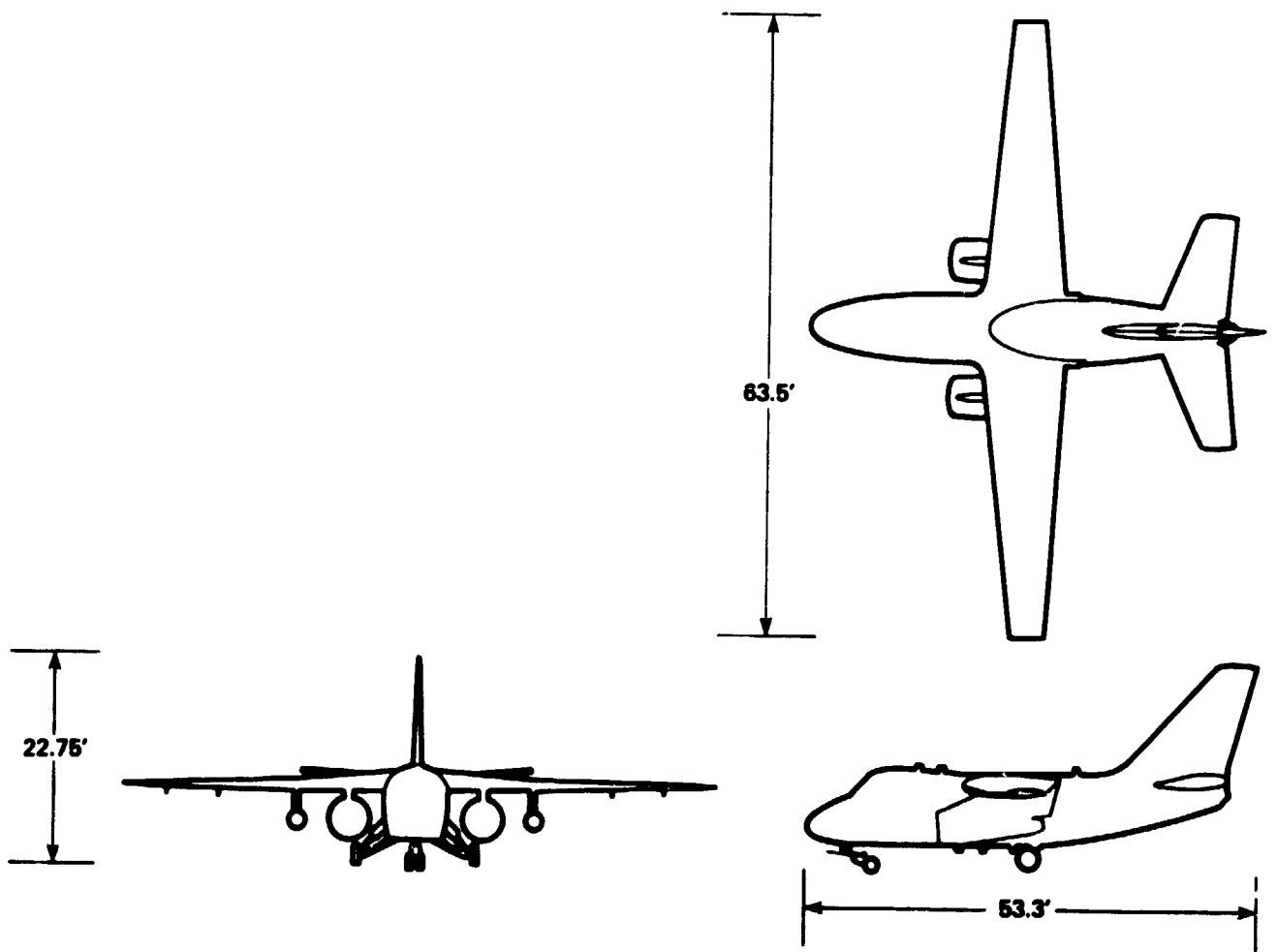


Figure 8. - S-3B Constrained Span Wing Design Outline Drawing

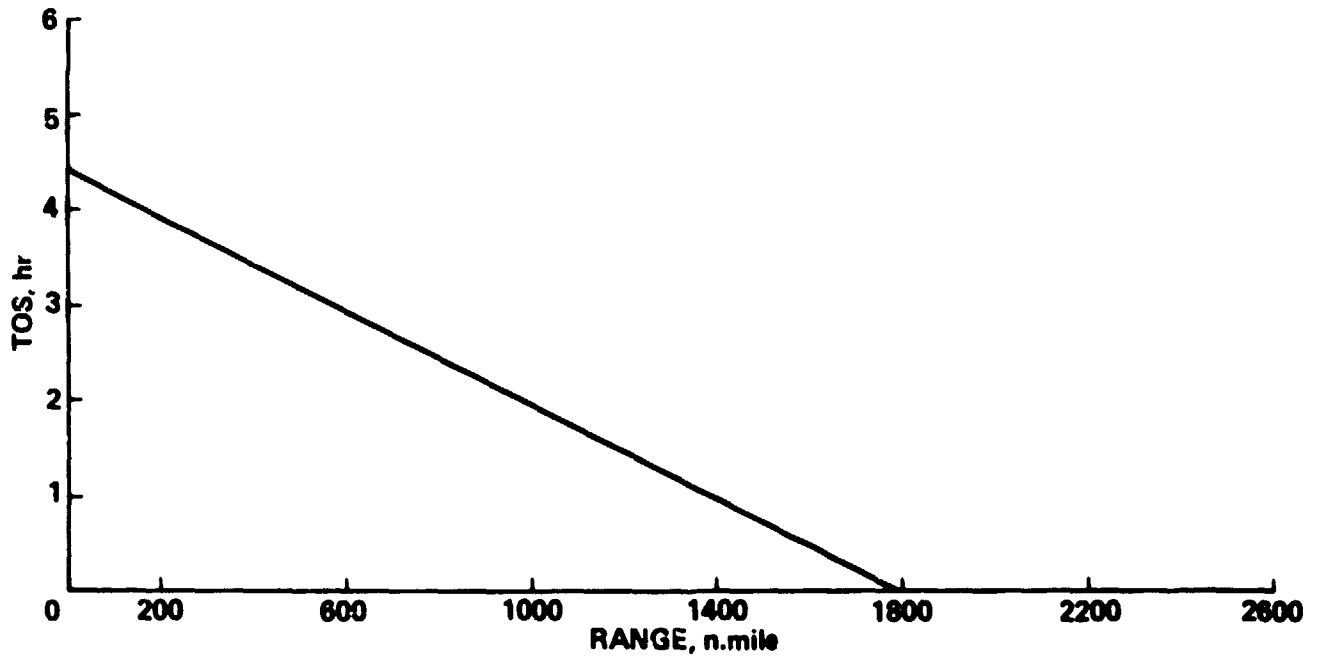
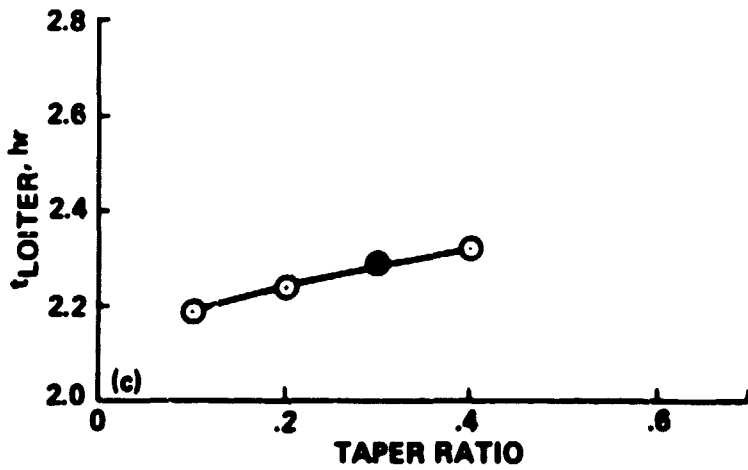
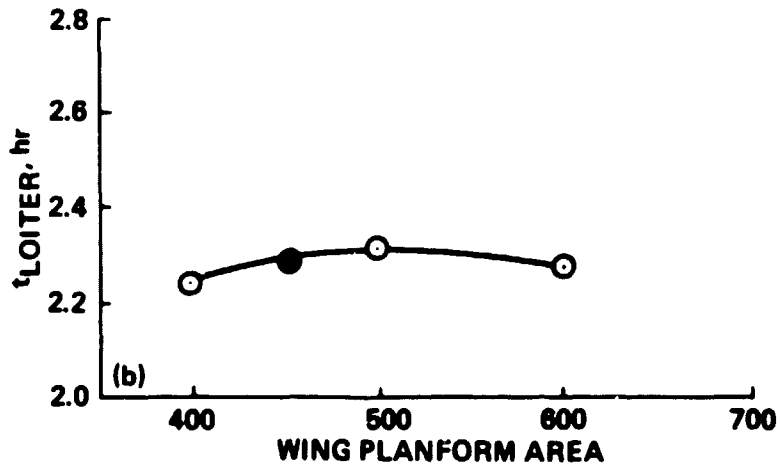
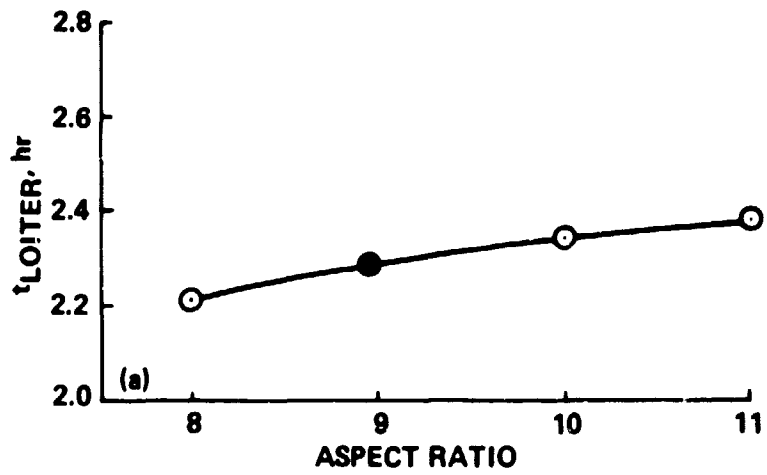


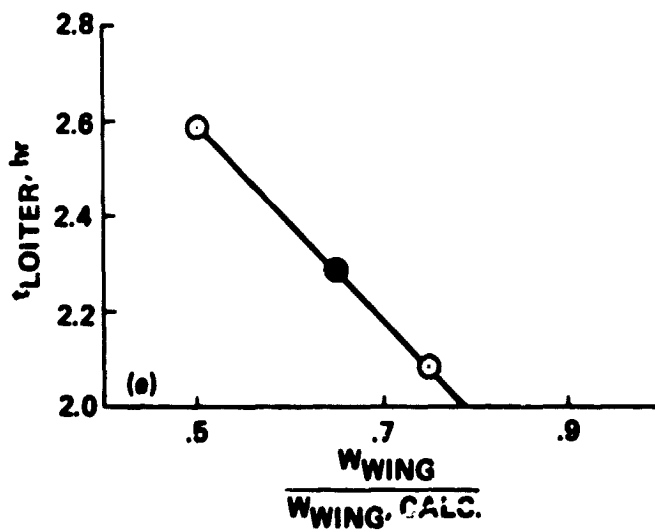
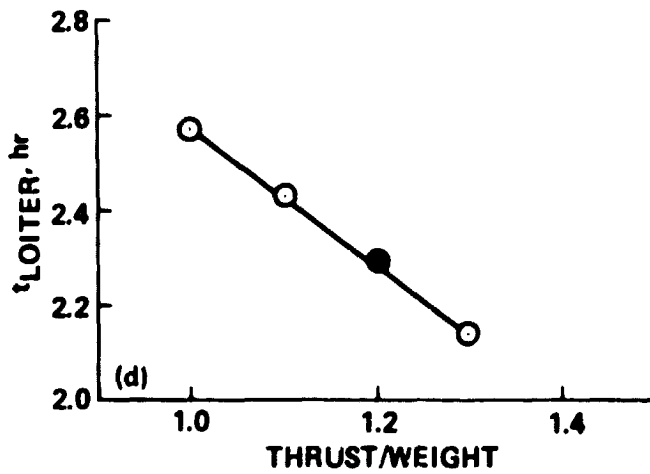
Figure 9. - Constrained Span Wing Design Range Vs. Time on Station



● = NOMINAL VALUE OF CONFIGURATION BEING STUDIED

O = VARIATION

Figure 10. - Constrained Span Wing Design Loiter Sensitivity



● = NOMINAL VALUE OF CONFIGURATION BEING STUDIED
 ○ = VARIATION

Figure 10 (Cont'd). - Constrained Span Wing Design Loiter Sensitivity

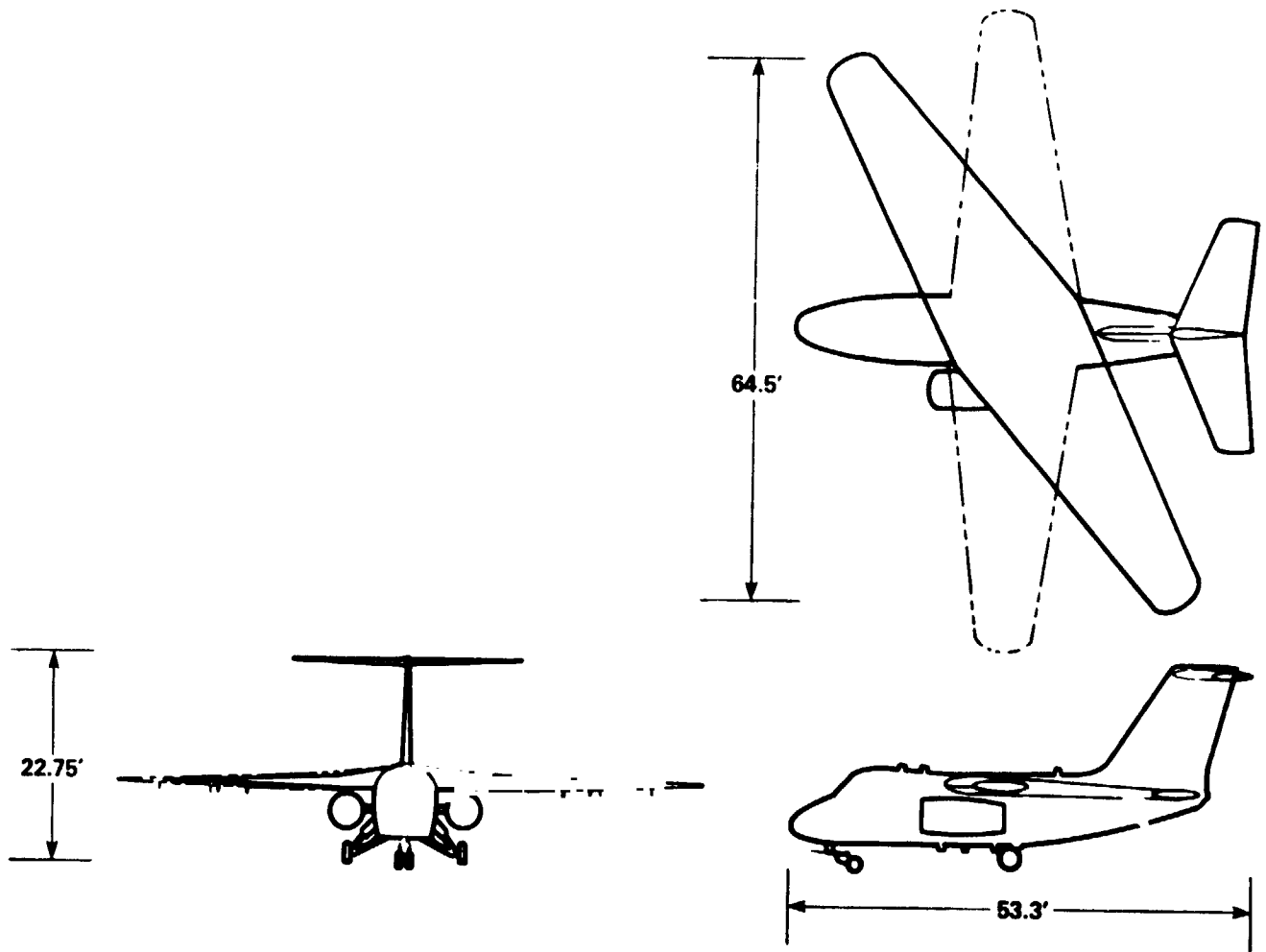


Figure 11. - S-38 Oblique Wing Design Outline Drawing

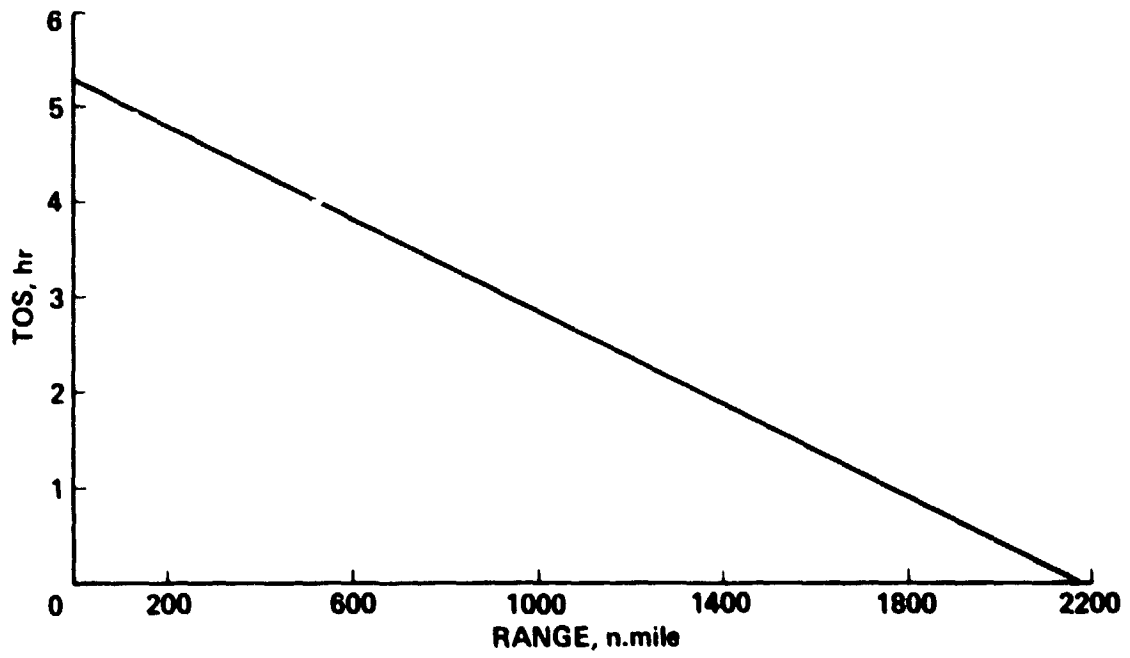
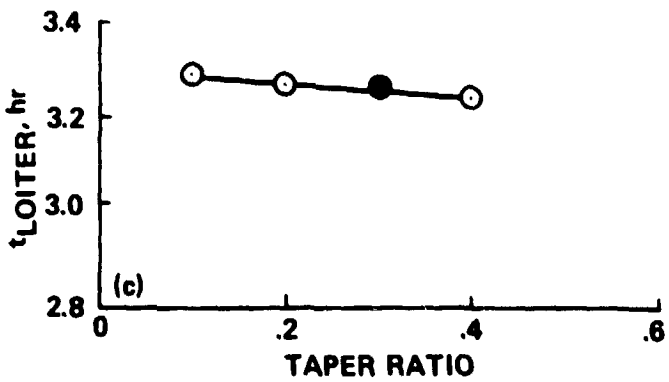
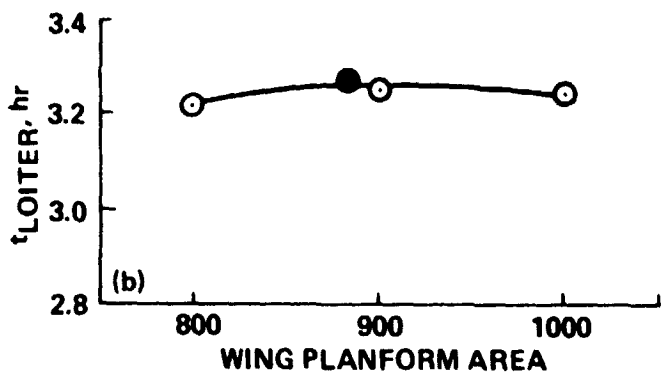
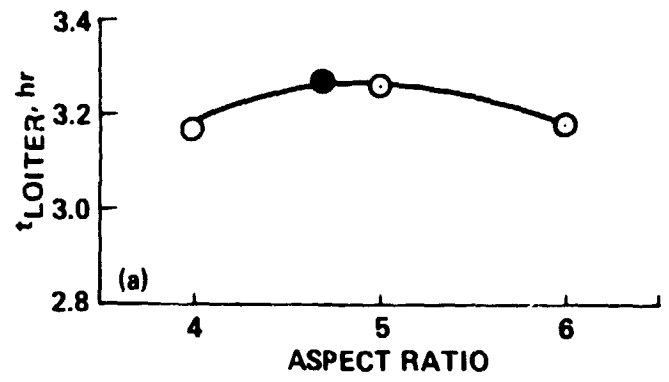
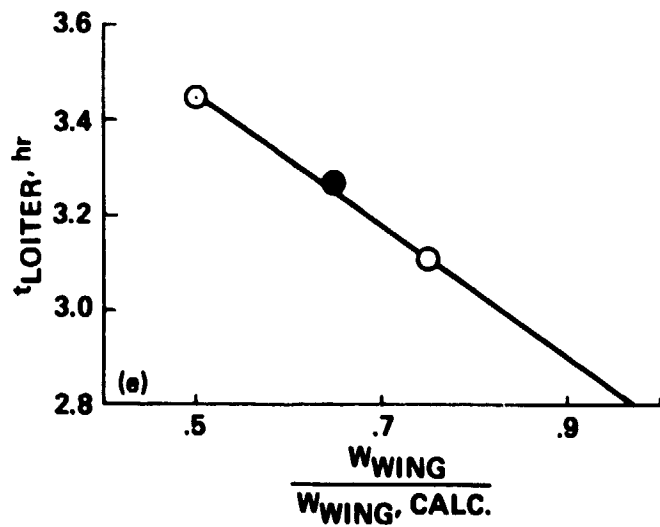
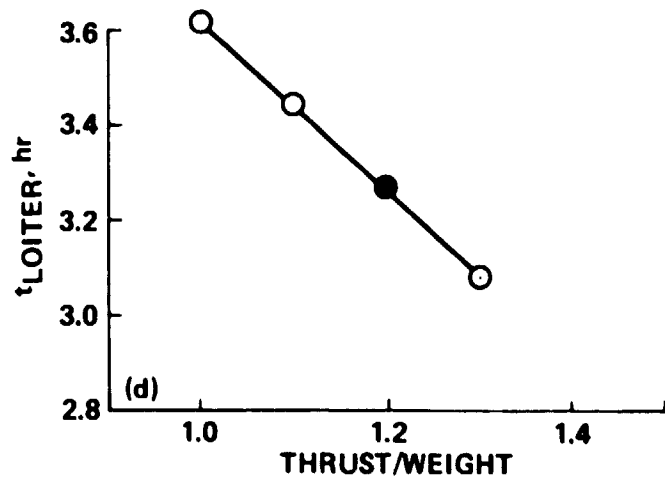


Figure 12. - Oblique Wing Design Range Vs. Time on Station



● = NOMINAL VALUE OF CONFIGURATION BEING STUDIED
 ○ = VARIATION

Figure 13. - Oblique Wing Design Loiter Sensitivity



● = NOMINAL VALUE OF CONFIGURATION BEING STUDIED

○ = VARIATION

Figure 13 (Cont'd). - Oblique Wing Design Loiter Sensitivity

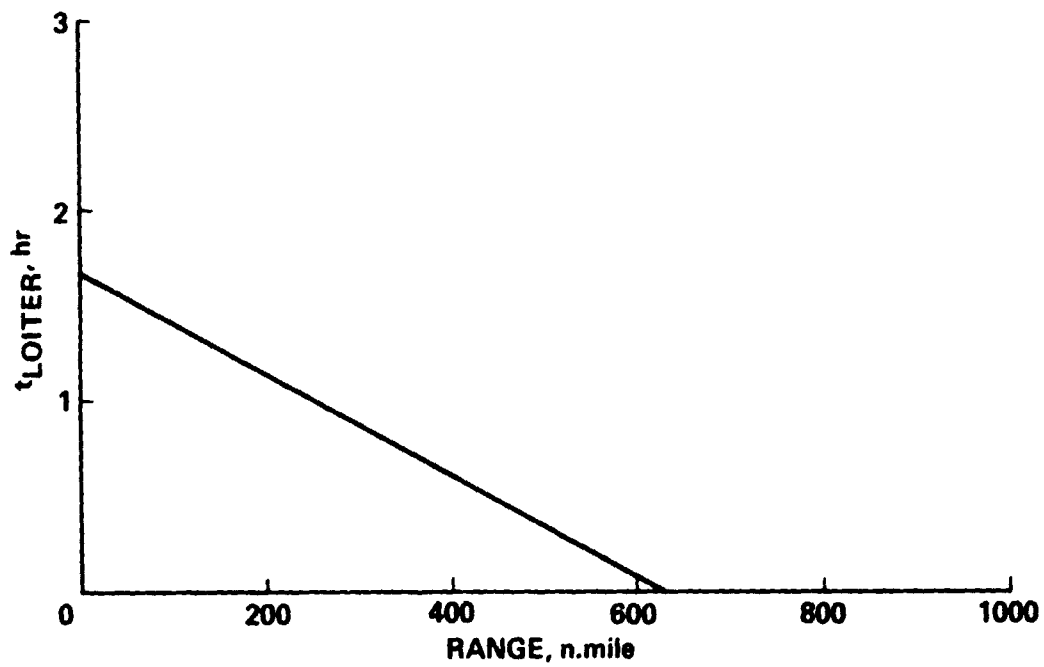


Figure 14. - S-3B/Pegasus Range Vs. TOS

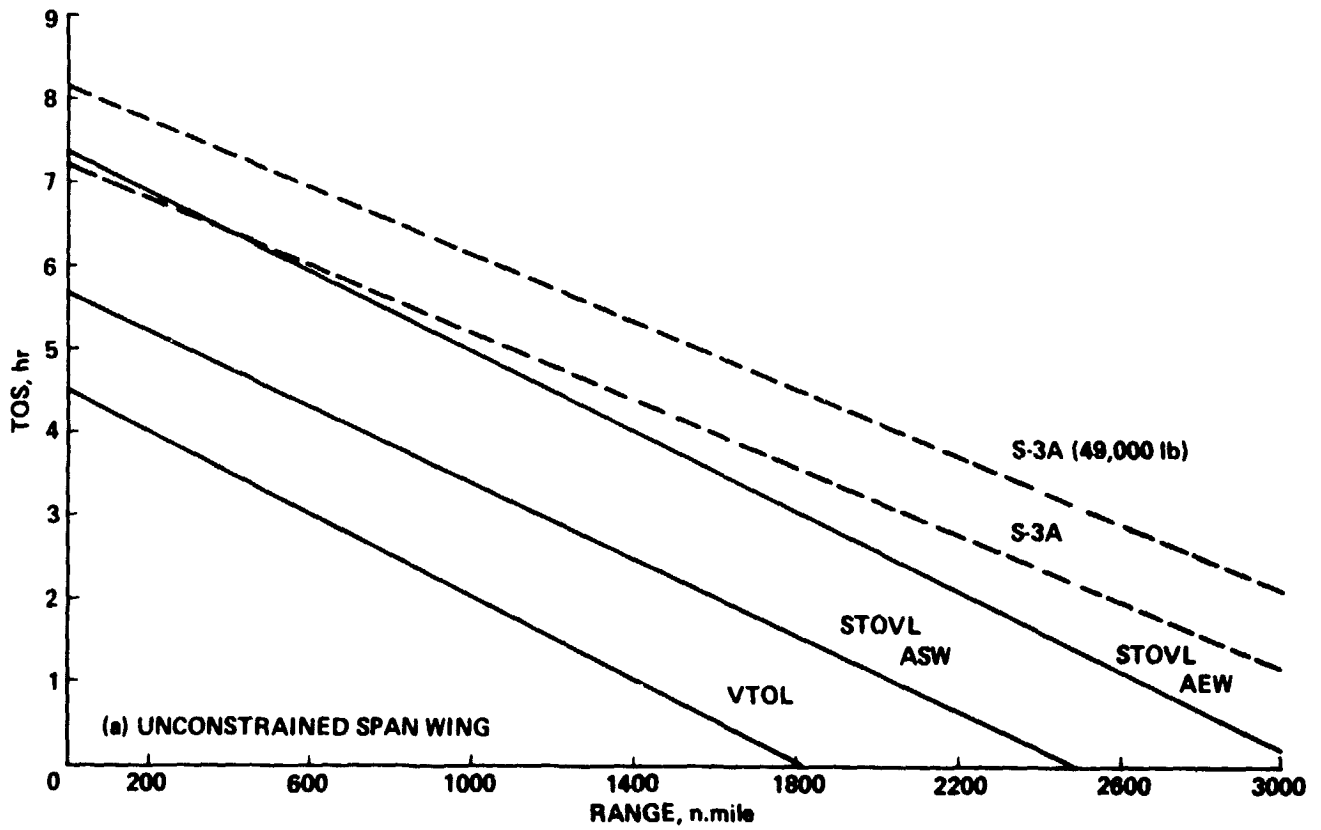


Figure 15. - Summary of Range Vs. TOS Results - S-3B
Unconstrained Span

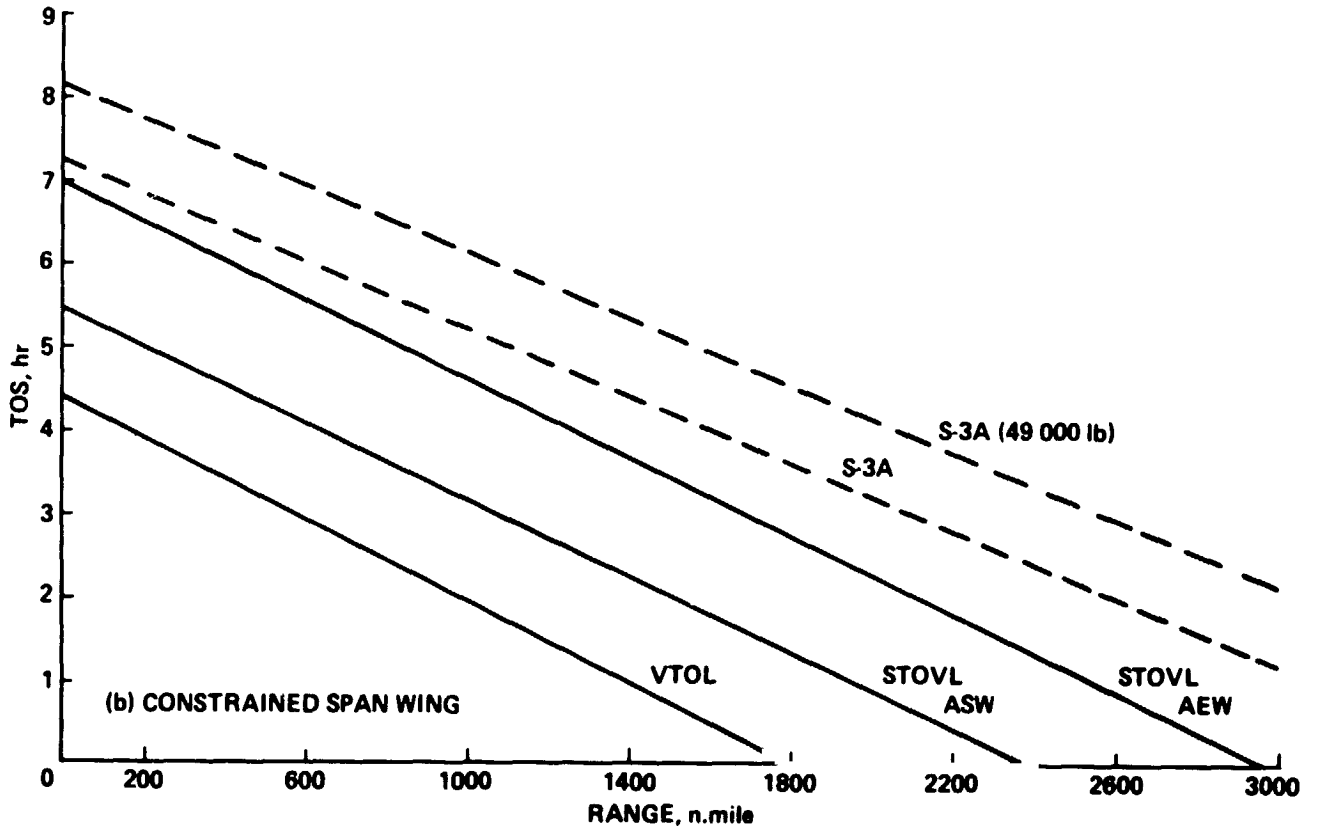


Figure 15 (Cont'd). - Summary of Range Vs. TOS Results - S-3B
Constrained Span

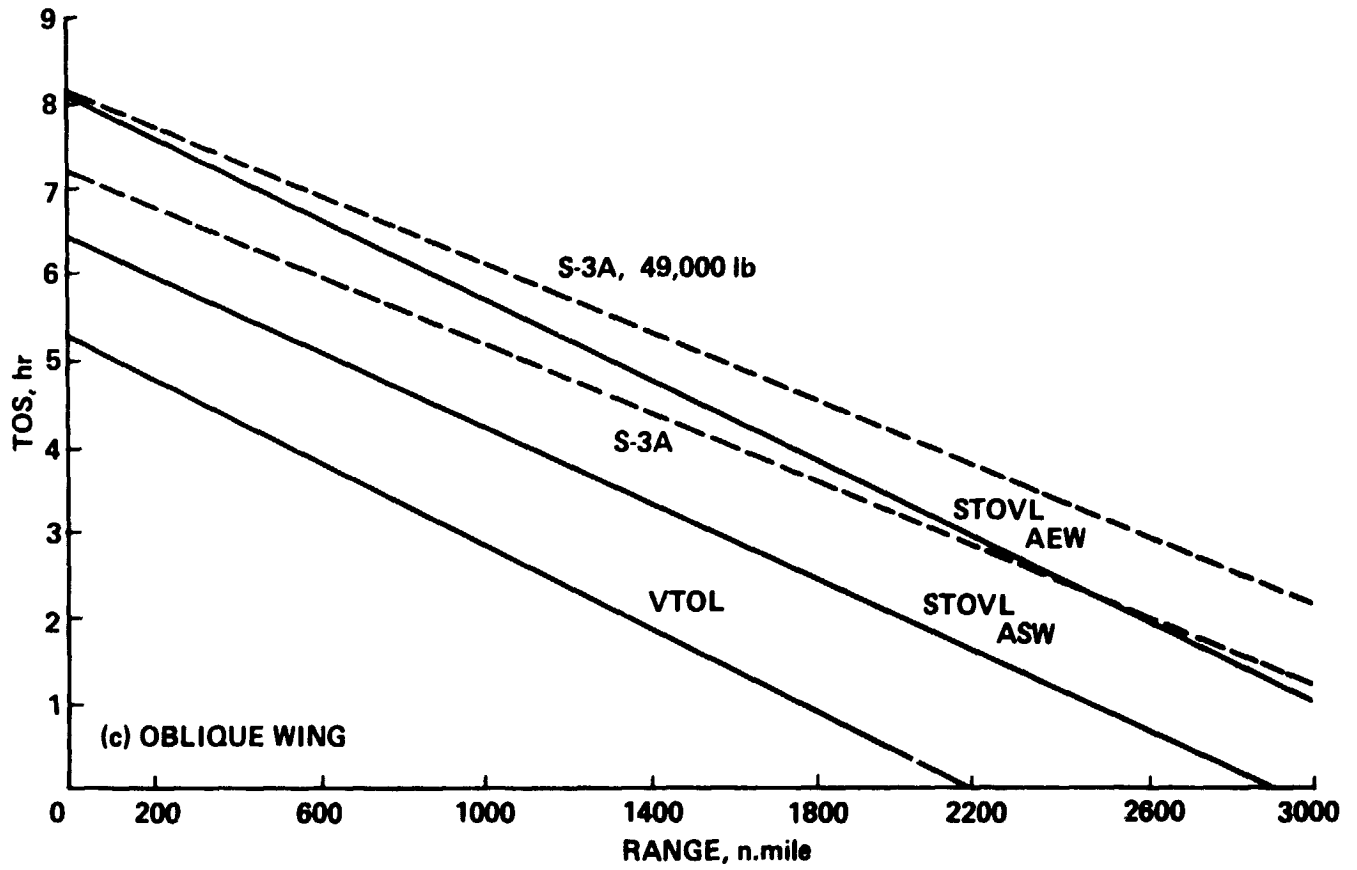


Figure 15 (Cont'd). - Summary of Range Vs. TOS Results - S-3B Oblique Wing